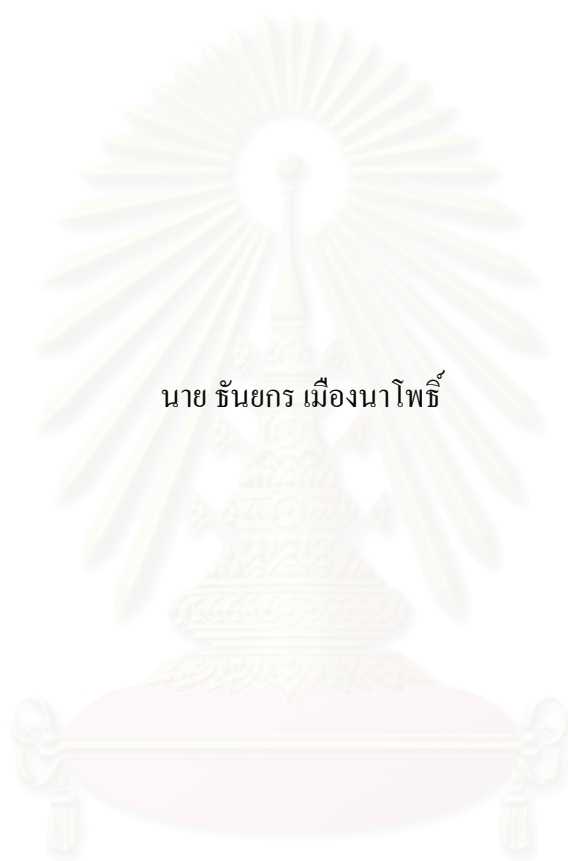การสังเคราะห์อนุภาคทองระดับนาโนเมตรด้วยการควบคุมความเป็นกรดด่างและการใช้คลื่นเสียงความถี่สูง

นาย ธันยกร เมืองนาโพธิ์

SYNTHESIS OF GOLD NANOPARTICLES USING pH CONTROL AND ULTRASONICATION

Mr. Tanyakorn Muangnapoh

A Thesis Submitted in Partial Fulfillment of the Requirements

for the Degree of Master of Engineering Program in Chemical Engineering

Department of Chemical Engineering

Faculty of Engineering

Chulalongkorn University

Academic Year 2007

Thesis Title	SYNTHESIS OF GOLD NANOPARTICLES USING pH CONTROL AND ULTRASONICATION
By	Mr. Tanyakorn Muangnapoh
Field of study	Chemical Engineering
Thesis Advisor	Associate Professor Tawatchai Charinpanitkul, D.Eng.

Accepted by the Faculty of Engineering, Chulalongkorn University in Partial Fulfillment of the Requirements for the Master's Degree

....Dean of the Faculty of Engineering

(Associate Professor Boonsom Lerdhirunwong, Dr.Ing)

THESIS COMMITTEE

.... Chairman

(Assistant Professor Varong Pavarajarn, Ph.D.)

.... Thesis Advisor

(Associate Professor Tawatchai Charinpanitkul, D.Eng.)

.... Member

(Professor Supot Hannongbua, Ph.D.)

.... Member

(Assistant Professor Bunjerd Jongsomjit, Ph.D.)

.... Member

(Assistant Professor Joongjai Panpranot, Ph.D.)

ธันยกร เมืองนาโพธิ์ : การสังเคราะห์อนุภาคทองระดับนาโนเมตรด้วยการควบคุมความเป็นกรดด่างและการใช้คลื่นเสียงความถี่สูง. (SYNTHESIS OF GOLD NANOPARTICLES USING pH CONTROL AND ULTRASONICATION)

อ. ที่ปรึกษา : รศ. ดร. ธวัชชัย ชรินพาณิชกุล จำนวนหน้า 80 หน้า.

อนุภาคทองระดับนาโนเมตรเป็นวัสดุระดับนาโนเมตรที่กำลังได้รับความสนใจเป็นอย่างมากเนื่องจากสามารถแสดงคุณสมบัติพิเศษที่แตกต่างออกไปจากทองที่พบตามธรรมชาติ โดยที่สมบัติทางแสงเป็นสมบัติหนึ่งที่มีความน่าสนใจมากที่สุด เนื่องจากสมบัติทางแสงของอนุภาคทองจะขึ้นอยู่กับขนาดของอนุภาคทองนั้นๆ การสังเคราะห์อนุภาคทองระดับนาโนเมตรนั้นสามารถทำได้หลายวิธี วิธีการทำปฏิกิริยารีดักชันในระบบของเหลวก็เป็นอีกวิธีหนึ่ง ซึ่งมีความได้เปรียบเนื่องจากใช้พลังงานน้อยและอุปกรณ์ที่ไม่ซับซ้อน

ในงานวิจัยนี้จึงตั้งเป้าหมายที่จะศึกษาผลกระทบของตัวแปรต่างๆที่มีผลต่อขนาดของอนุภาคทอง ได้แก่ อัตราส่วนโดยโมลของสารตั้งต้น และตัวรีดิวซ์ ความเข้มข้นโดยรวมของสารตั้งต้น อุณหภูมิที่ใช้ในการทำปฏิกิริยา กำลังในการโซนิคเคชั่นและความเป็นกรดด่าง จากผลการทดลองพบว่า ขนาดของอนุภาคทองระดับนาโนเมตรจะขึ้นอยู่กับอัตราส่วนโดยโมลของสารตั้งต้น (HAuCl$_4$) และตัวรีดิวซ์ (Na$_3$C$_6$H$_5$O$_7$) ความเข้มข้นโดยรวมของสารตั้งต้นและอุณหภูมิที่ใช้ในการทำปฏิกิริยา ในขณะที่กำลังในการโซนิคเคชั่นไม่ส่งผลต่อขนาดของอนุภาคทองระดับนาโนเมตร นอกจากนี้ขนาดและเสถียรภาพของอนุภาคทองระดับนาโนเมตรนั้นสามารถควบคุมได้โดยการปรับค่าความเป็นกรดด่างของสารละลาย

สืบเนื่องจากคุณสมบัติทางด้านไฟฟ้า อนุภาคทองระดับนาโนเมตรจึงเป็นอีกทางเลือกหนึ่งเพื่อนำมาใช้เป็นโอโซนเซนเซอร์ จากผลการทดลองในงานวิจัยนี้พบว่าการที่โมเลกุลของโอโซนถูกดูดซับบนแผ่นฟิล์มของอนุภาคทองระดับนาโนเมตรส่งผลให้เกิดการเปลี่ยนแปลงความต้านทานไฟฟ้าของอนุภาคทองระดับนาโนเมตร

ภาควิชา........วิศวกรรมเคมี.................. ลายมือชื่อนิสิต....ธันยกร เมืองนาโพธิ์....

สาขาวิชา.......วิศวกรรมเคมี.................. ลายมือชื่ออาจารย์ที่ปรึกษา.....................

ปีการศึกษา.....2550.................. ลายมือชื่ออาจารย์ที่ปรึกษาร่วม.....................

4870318021   : MAJOR CHEMICAL ENGINEERING

KEY WORD: GOLD NANOPARTICLES / MOLAR RATIO / SONICATION / pH / STABILITY/OZONE SENSOR

TANYAKORN MUANGNAPOH: SYNTHESIS OF GOLD NANOPARTICLES USING pH CONTROL AND ULTRASONICATION. THESIS ADVISOR: ASSOC. PROF. TAWATCHAI CHARINPANITKUL, D.Eng., 80 pp.

Gold nanoparticle is a nanomaterial drawing many research attentions because it could exhibit distinctive properties, which are different from its bulk. Optical property is the most interesting aspect because it is strongly dependence on size of gold nanoparticles which could be controlled by many parameters. Though gold nanoparticles could be synthesized by various methods, liquid-phase reduction method is recognized as one of the most potential method because it consumes less energy and uses simple apparatus.

Hence this research sets its aim at investigating the dependence of gold nanoparticle size on the molar ratio of precursor and reducing agent, total concentration of precursors, reaction temperature, sonication power and pH. Based on our experimental results, size of gold nanoparticle was strongly dependent on the molar ratio of precursor ($HAuCl_4$) to reducing agent ($Na_3C_6H_5O_7$), total concentration of precursors and reaction temperature while sonication power could provide insignificant effect on the size of gold nanoparticles. Moreover, size and stability of gold nanoparticles could be controlled by adjusting pH of solution.

Regarding to electrical property, gold nanoparticle is another alternative for using as ozone sensor. In this research, it was experimentally found that adsorption of ozone molecules on gold nanoparticles film caused a change of electrical resistance of gold nanoparticles.

Department........Chemical Engineering...... Student's signature...Tanyakorn Muangnapoh...

Field of study.....Chemical Engineering...... Advisor's signature....................................

Academic year.......2007................

ACKNOWLEDGEMENTS

CONTENTS

III FUNDAMENTAL KNOWLEDGE

IV EXPERIMENTAL

LIST OF TABLES

LIST OF FIGURES

Page

NOMENCLATURES

A	Hamaker constant
c_i	Concentration of species
CNTs	Carbon nanotubes
DLS	Dynamic light scattering
F.C.C.	Face centered cubic
I	Ionic strength
MAW	Maximum Absorption Wavelength
r	Radius
S	Distance
TEM	Transmission Electron Microscope
UV-Vis	Ultraviolet and visible
z_i	Valencies of species
ε	Energy in balance conditions
ε_0	Permittivity of vacuum
ε_r	Dielectric constant
Φ_A	Van der Waals interactions potential
Φ_{DLVO}	Total interaction potential
Φ_{LJ}	Lennard-Jones potential
Φ_R	Electrical repulsion potential
σ	Interatomic distance
ζ	Zeta potential
κ	Debye length

CHAPTER I

INTRODUCTION

1.1 Background

"Why cannot we write the entire 24 volumes of the Encyclopedia Britannica on the

head of a pin?"

There's Plenty of Room at the Bottom

Richard P. Feynman

This is a famous speech that Richard Feynman gave on December 29th, 1959 at the annual meeting of the American Physical Society. It inspires many researchers to focus on nanoscale investigation and it was recognized as the beginning of global attention to study nanotechnology.

Nowadays, research works on nanomaterials are becoming of interest owing to their novel physical and chemical attributes. Gold nanoparticle is a nanomaterial drawing many research attentions because of their promising properties, which are different from its bulk. In its bulk form, gold is the most stable metal, which is inert, soft, golden yellow metal with having a face centered cubic structure (F.C.C.), and a melting point of 1068 ^{O}C (Corti, Holliday, and Thompson, 2004). This structure of gold is shown in Figure 1.1. At the nanoscale level, gold nanoparticle shows different color appearance and provides many potential applications in electronics, catalytic, biomedical, coating and decorative.
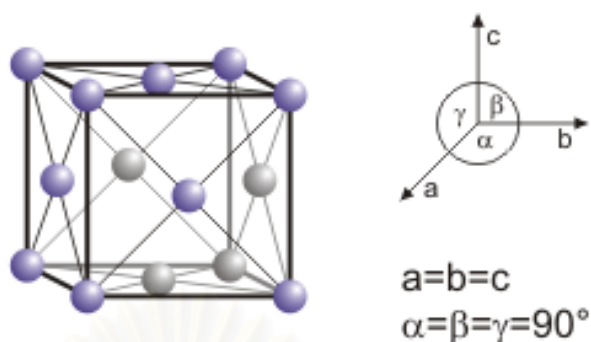
Figure 1.1 Face centered cubic structure of gold

There are many ways, such as arc discharge (Lin et al., 2006), photochemistry (Pal et al., 2001; Pal et al., 2005; Pal et al., 2007), radiolysis (Henglein and Meisel, 1998), and reverse micelles (Scaffardi et al., 2005) to synthesize gold nanoparticles. Nevertheless, these methods require sophisticated apparatus, which lead to there limitation for large scale production.

However, there are two well-known methods that employ less energy and simple apparatus for preparing gold nanoparticles and its derivatives. The first one is Turkevitch method. It is a conventional technique for synthesis of aqueous gold nanoparticles by the reduction reaction of auric chloride with trisodium citrate which was proposed by Turkevitch in 1951 (Turkevitch, Stevenson, and Hillier, 1951). With this method, the citrate salt acts as the reducing agent to reduce Au^{3+} to Au^0 and the stabilizing agent by forming a layer of citrate ions over gold nanoparticles surface, inducing enough electrostatic repulsion between individual particles to keep them well dispersed in the medium. A particle size obtained is about 20 nm. This method gives uniform and fairly spherical nanoparticles. The second one is Brust-Schiffrin method. This method was discovered by Brust and Schifrinn in 1994 (Brust et al., 1994). They produced gold nanoparticles in organic liquids that are normally not

miscible with water (two-phase synthesis) with thiols as a stabilizer. Nanoparticles show that they have diameters in range of 1-3 nm and a maximum particle size distribution at 2.0-2.5 nm. However, nanoparticles prepared by this method cannot be used in wide applications due to existence of functionalized thiols on gold surface.

To the best of our knowledge, the formation of gold nanoparticles and the stability of gold colloid have not been thoroughly investigated. In such situation, this research is focusing on controlling the size of gold nanoparticles which could be synthesized by Turkevitch method and applying ultrasonic technique and pH control to decrease the size of gold nanoparticles and improve the stability of gold colloid with measuring zeta potential and absorption spectra of colloid. Moreover, this research also investigates the availability of synthesized gold nanoparticles for applying to make a gas sensor.

1.2   Objectives

This research sets its objective to investigate factors which affect on the formation of gold nanoparticles and the stability of gold colloid.

1.3   Scopes of Research

1. To investigate the formation of gold nanoparticles synthesized by Turkevitch method with variation of the following parameters:

       1.1   Molar ratio of precursor (HAuCl$_4$) to reducing agent (Na$_3$C$_6$H$_5$O$_7$) (1:1-1:20)

       1.2   Total concentration of precursors (3.1x10^{-3} - 7.6x10^{-2} mol/dm^3)

1.3 Reaction temperature (60-100 ^{O}C) controlled by temperature controller

1.4 Sonication power supplied by ultrasonic homogenizer (0-35 W)

2. To investigate the stability of gold colloid by varying pH of solution in a range of 3-10

3. To explore possibility of applying synthesized gold nanoparticles as ozone sensor

1.4 Expected Benefits

1. To understand the formation of gold nanoparticles which synthesized by Turkevitch method and effects of various parameters on size, morphology and stability of gold nanoparticles

2. To improve a stability of gold colloid because an aggregation of gold nanoparticles will not occur if there is an optimal condition is prepared to add a suitable amount of ions around particles

3. Knowledge of gas sensor which made from nanomaterials and availability of using gold nanoparticles as gas sensor

CHAPTER II

LITERATURE REVIEW

2.1 Synthesis of gold nanoparticles in one-phase liquid

Turkevitch et al. (1951) studied the reduction reaction of auric chloride with trisodium citrate. With this method, the citrate salt acted as the reducing agent to reduce Au^{3+} to Au^0 and then it also acted as the stabilizing agent by forming a layer of citrate ions over gold nanoparticles surface, inducing enough electrostatic repulsion between individual particles to keep them well dispersed in the medium. This method gave uniform and fairly spherical nanoparticles (~20 nm)

Fren (1973) furthered conduted investigation of Turkevitch by studying the effect of molar ratio between the reducing agent (trisodium citrate) and gold solution. The result showed that the size of obtained gold nanoparticles was 16-147 nm.

Yonezawa and Kunitake (1999) proposed a practical preparation of sodium 3-mercaptopropionate-stabilized gold nanoparticles by simultaneous adding of citrate salt and surfactant. The size could be controlled by varying the stabilizer/gold ratio. They found that synthesized gold nanoparticles were in a range of 2-20 nm.

Sastry et al. (2002) studied the synthesis of gold nanoparticles of good monodispersity by the reduction of aqueous chloroaurate ions by the amino acid,

aspartic acid. The colloidal gold solution thus formed was extremely stable in time, indicating electrostatic stabilization via nanoparticle surface-bound amino acid molecules. This observation has been used to modulate the size of the gold nanoparticles in solution by varying the molar ratio of chloroaurate ions to aspartic acid in the reaction medium. They found that synthesized gold nanoparticles were in a range of 24-42 nm.

Dravid et al. (2004) proposed a one-step process for synthesizing water-dispersed spherical gold nanoparticles using the multifunctional molecule oleyl amine (OLA). Synthesized gold nanoparticles were in a range of 10-75 nm. The particle size and distribution of gold nanoparticles was strongly controlled by the amine:gold ion molar ratio.

Okubo, Hu, and Yamaguchi (2004) studied the synthesis of gold nanoparticles using gold solution, trisodium citrate, tannic acid and using 1-mercapto-3,6,9-trioxodecane as stabilizer. The size of obtained gold nanoparticles was around 10 nm

Dai et al. (2005) proposed a method for direct synthesis of amine-stabilized gold nanoparticles by using 3-(trimethoxysilylpropyl)diethylenetriamine (TMSP dien). The amine groups of this bifunctional molecule acted as a stabilizer for gold nanoparticles as they formed by reduction of $HAuCl_4$. Highly stable gold nanoparticles with sizes tunable between 8 and 20 nm can be readily obtained.

Dutta and Sugunan (2005) studied synthesis of glutamate functionalized single crystal gold nanoparticles by reducing a solution of chloroauric acid with monosodium glutamate. Highly uniform size distributions of the nanoparticles can be obtained by having an excess of monosodium glutamate in the starting solution. The result of this result was similar to the conventional synthesis of gold nanoparticles by reduction of chloroauric acid with trisodium citrate (Turketvitch method), the obtained particle sizes were varied in the range of 14 – 25 nm without loosing the uniformity in its size distribution by varying the concentration of the reducing agent.

Dutta et al. (2005) proposed a novel strategy for detection of heavy metal ions in water by using 20 nm gold particles capped with a biopolymer called chitosan. Polymer capping of nanoparticles serves a two-fold purpose, that of stabilization and surface functionalization for application as sensors.

Huang and Yang (2005) studied the size control synthesis of gold nanoparticles under mild conditions by reducing $HAuCl_4$ with 3-thiopheneacetic acid (TA). TA also acted as a protecting agent by loosely absorbing on the surface of produced Au^0. With a relative higher concentration of TA or under a lower temperature, only spherical gold nanoparticles were formed. While lowering the concentration of TA, increasing the molar ratio of TA to gold, or increasing the reaction temperature, larger gold particles both in spherical and polygonal could be obtained. The result showed that the size of obtained gold nanoparticles was in a range of 10-50 nm.

Khanna et al. (2005) prepared poly(vinyl alcohol) (PVA) stabilized gold nanoparticles in aqueous medium by using two different reducing agents; hydrazine hydrate, a stronger reducing agent and sodium formaldehydesulfoxylate (SFS), a slightly weaker reducing agent. SFS was used for first ever time for reduction of gold metal salt. The PVA stabilized gold nanoparticles solutions were wine red to blood red coloured and stable over a long period of time with no indication of aggregation. The solution showed strong visible light absorptions in the range of 520–540 nm, characteristics of gold nanoparticles. Transmission electron microscopy (TEM) of a more than two-week-old sample revealed well-defined non-agglomerated spherical particles of about 50 nm diameter in solutions.

Song, Kim, and Kim (2006) studied the synthesis of gold nanoparticles using N,N-dimethyllacetoacetamide at room temperature. The result showed that the size of obtained gold nanoparticles was 20-100 nm.

Luo (2007) prepared gold nanoparticles through a one-step route, carried out by mixing 3-thiophenemalonic acid and $HAuCl_4$ aqueous solutions without the additional step of introducing other reducing agents and protective agents. The growth of such gold nanoparticles followed the Ostwald ripening growth mechanism. Synthesized gold nanoparticles with size of 2-20 nm were obtained.

2.2 Synthesis of gold nanoparticles in two-phase liquid

Brust et al. (1994) used two phase (water-toluene) reduction of $AuCl_4^-$ by sodium borohydride in the presence of an alkanethiol and reported that excellent

control and uniformity of size can be achieved since the protective capping agent (usually a thiol) was chemically bound by a coordinate bond to the surface of gold nanoparticles. Size of synthesized gold nanoparticles was around 2 nm.

Bhattacharya and Srivastava (2003) followed the Brust method to synthesize gold nanoparticles and used a metal-chelator derivative as stabilizer. A transmission electron micrograph showed that gold nanoparticles in the sample were of 3–10 nm diameters.

Mareno-Mañas, Pleixats, and Tristany (2005) studied reduction of gold (III) species in two-phase fluorous-organic solvent system and stabilized gold nanoparticles by using compounds with long perfluoroalkyl chains. Size of obtained gold nanoparticles was in a range of 2.5-40 nm.

Wang et al. (2005) used poly (benzyl ether) alcohol dendrons (G_n–OH, n = 1–3 as a stabilizing medium in the preparation of gold nanoparticles. The G_n–Au nanoparticle composites are stable and resist aggregation at room temperature. Varying the generation number of dendrons, concentration of precursor and reduction agent, can control the size and shape of the nanoparticles. The gold nanoparticles were fairly uniform and range in size from 8 to 15 nm.

2.3   Other method to synthesize gold nanoparticles

2.3.1   Arc discharge

Lin et al. (2006) prepared gold nanoparticles by arc discharge in water. It was proposed for the first time. Fabrication of gold nanostructures in deionized water has been successfully established. Size of synthesized gold nanoparticles was in a range of 15-30 nm.

2.3.2   Photochemistry

Pal et al. (2001) synthesized gold nanoparticles with prechosen size ranging from 5 to 110 nm by photochemistry method. Firstly, small spherical particles (seed) of average diameters between 5 and 20 nm were prepared by varying the ratio of gold ion concentration to stabilizer/reductant, TX-100 concentration and using UV irradiation. Secondly, 20–110 nm particles were formed by a non-iterative seed-mediated growth where small particles produced by the above irradiation technique were exploited as seeds and fresh Au (III) ions were reduced onto the surface on the seed particles by ascorbic acid.

Pal et al. (2005) used UV photoactivation technique for the preparation of gold nanoparticles using sodium alginate, a carbohydrate-based biopolymer. Sodium alginate acted both as a reducing agent and as a stabilizer. The size of the particles depended on the concentration of the polymer. Produced gold particles were spherical, very stable and were encapsulated by the polymer. These particular gold particles may be useful for biological applications because of the biocompatibility of

sodium alginate. The result showed that the size of produced gold nanoparticles was 9-14 nm.

Pal et al. (2007) proposed a new method to synthesize cubic gold nanoparticles. A chiral reagent, 2-naphthol, has been introduced under alkaline solution as a reductant for $HAuCl_4$ in CTAB micelle to produce exclusively cubic gold nanoparticles under UV photoactivation. Prolonged irradiation helped the digestion of the primarily evolved spherical particles into smaller gold nanocubes, which then acted as tiny cubic seeds, leading to the formation of larger nanocubes. The smaller cubes took the assistance of CTAB under alkaline condition to serve as the seed in directing the transformation of all the spherical colloids into cubic shapes under continuous irradiation via Ostwald ripening. The TEM analysis at this stage indicated that the cubes have a mean edge length 40 ± 5 nm.

2.3.3 Radiolysis

Henglein et al. (1998) proposed a mechanism in which the radicals transferred electrons to the gold particles and $Au(CN)_2^-$ was subsequently reduced by the stored electrons directly at the surface of the particles. In further steps of particle enlargement, $Au(CN)_2^-$ was reduced in solutions which the synthesized gold particles served as seeds, the result being larger and larger gold particles up to 120 nm. This method claimed that the radiation chemical method was possible to enlarge gold particles to any desired size.

2.3.4 Reverse micelles

Scaffardi et al. (2005) synthesized gold nanoparticles in 'reverse micelles' in water–hydrocarbon phases and isolated with a stabilizer. The solvent was n-heptane and the water was triply distilled. Sodium bis (2-ethylhexyl) sulfosuccinate was used as surfactant and N-[3-(trimethoxysilyl)propyl]diethylenetriamine as stabilization agent. Size of gold nanoparticles synthesized by this method was 1-2 nm.

2.4 Effect of molar ratio on synthesis of gold nanoparticle

Most of researchers mentioned above used molar ratio of gold solution to reducing agent between 1:1 and 1:20. They found that the more molar ratio the smaller particle size and spherical shape were obtained.

2.5 Effect of temperature on synthesis of gold nanoparticle

Turkevitch et al. (1951) found that lowering the temperature by 10 ^{O}C increased by a factor of the two the time necessary for the completion of the reaction as judged by the deepening of color. Both the mean particle size and the root mean square deviation decreased slightly with decreasing temperature.

Goia, Andreescu, and Sau (2006) found that a shorter wavelength of maximum absorption of gold particles was obtained when reaction temperature increased. The particle size decreased because of faster reactions in homogeneous phase and nucleation at higher temperature.

2.6 Effect of sonication power on synthesis of gold nanoparticle

Atobe, Park, and Fuchigami (2005) studied the effect of concentration of stabilizer (sodium dodecylsulfate: SDS) and ultrasonic power on the formation of gold nanoparticles. They found that gold nanoparticles with multiple shape and size were synthesized by controlling the concentration of stabilizer and ultrasonic power. The more ultrasonic power the smaller size and spherical shape were obtained.

2.7 Effect of pH on synthesis of gold nanoparticle

Toshima, Shiraishi, and Arakawa (2002) claimed that gold nanoclusters protected by 3-mercaptopropionic acid (MPA-Au nanoclusters) were prepared by citrate-reduction of hydrogen tetrachloroaurate(III) in the presence of sodium   3-mercaptopropionate. Color of the dispersions of MPA-Au nanoclusters changed from red to purple by addition of hydrochloric acid and returned from purple to red by addition of an aqueous sodium hydroxide solution. The size of synthesized gold nanoparticle was in a range of 2-4 nm.

Goia, et al. (2006) studied the synthesis of stable dispersion of uniform gold nanoparticles at ambient temperature by mixing gold solution and iso-ascoebic acid. They found that the size of resulting nanoparticles is affected by the concentration and the pH of gold solution. The more pH value (base) the less zeta potential value was obtained. The gold nanoparticles size is around 25 nm.

CHAPTER III

FUNDAMENTAL THEORY

3.1 Colloid

In general, a colloid or colloidal dispersion is a two-phase system which exhibits intermediate behavior of between homogeneous and heterogeneous mixtures. Many familiar substances, including butter, milk, cream, aerosols (fog, smog, smoke), asphalt, inks, paints, glues and sea foam, are colloids. This field of study was introduced in 1861 by Scottish scientist Thomas Graham.

Size of dispersed particles recognized as colloid ranges from 0.001 to 1 micrometer. Dispersions of such the particle are referred to colloidal aerosols, colloidal emulsions and colloidal foams. Colloids may exhibit color or translucence because of the Tyndall effect. The Tyndall effect is the scattering of light by particles in the colloid. Colloids classification is shown in Table 3.1.

Table 3.1 Classification of colloid

		Dispersed phase		
		Gas	Liquid	Solid
Continuous Phase	Gas	None: all gases are soluble	Liquid aerosol, Examples: fog, mist	Solid aerosol, Examples: Smoke, dust
	Liquid	Foam, Examples: Whipped cream	Emulsion, Examples: Milk, mayonnaise, hand cream, blood	Sol, Examples: Paint, pigmented ink
	Solid	Solid foam, Examples: Aerogel, Pumice, Styrofoam	Gel, Examples: Gelatin, jelly, cheese,	Solid sol, Examples: Cranberry glass, Ruby glass

3.2 Colloid stability

Figure 3.1 illustrates a particle in water and associated in electric field. Most mineral particle surfaces are negatively charged, due to defects in the solid crystal lattice, chemical reactions at the surface, slightly soluble ions dissolving from the crystal and adsorption (and exchange) of ions from the surrounding solution. Some biological particles may be positively charged. The charge on the particle surface gives rise to ions of counter charge strongly bound to the surface. The total depth of strongly bound ions to the particle is called the Stern layer. At some distance further away from the particle there is the shear plane, which marks the start of diffuse layer. It is not possible to shear the ions off the particle that are closer to it than shear plane. Thus, if the particle surface potential will be measured at the shear plane, and not the true potential on the particle. This is called the *Zeta potential*. So, a particle in an electrolyte solution contains a strongly bound layer and a diffuse layer of ions close to its surface. This is known as the *Double layer*.
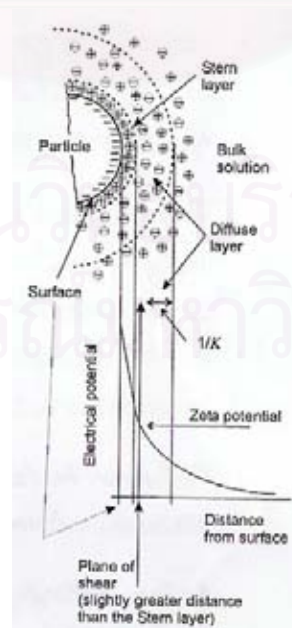
Figure 3.1 Electrical charges around a particle in an electrolyte solution

Colloid stability can be most easily understood in terms of the forces between a pair of particles - the interparticle pair potential. In fact, what we consider is the effective potential energy interaction between the two colloidal particles, averaged over all the degrees of freedom of the solvent molecules. This effective interaction is similar to the interaction between two molecules in a gas.

3.2.1 Molecular interactions

A simple pair potential, which describes the interaction potential energy between two identical gas molecules (or atoms) at distance r, is the Lennard-Jones potential, given by equation (3.1)

$$\Phi_{LJ} = 4\varepsilon \left[\left(\frac{\sigma}{r} \right)^{12} - \left(\frac{\sigma}{r} \right)^{6} \right] \qquad (3.1)$$

Where, σ and ε are interatomic distance and energy in balance conditions, respectively. Both σ and ε are constant values determined by molecular species. r is interatomic distance.

The r^{-6} term represents the van der Waals attraction between the molecules, arising from fluctuating dipoles due to the motion of outer electrons of the two molecules. These attractions lead to a decrease in energy. The r^{-12} term models repulsions at short distance, due to overlap of electron clouds. The repulsions lead to an increase in energy. The energy at infinite distance is defined as zero.

The simplest way of calculating the interaction potential energy between two particles in a colloidal dispersion is to assume that every molecule in the particle interacts with every other molecule (both in the solvent, the particle itself, and the

other particle). The resultant balance of attractive and repulsive forces dictates the physical properties and stability of the colloidal system.

3.2.2 Van der Waals attraction

When particles are small, typically in micrometers or less, and are dispersed in a solvent, van der Waals attraction force and Brownian motion play important roles, whereas the influence of gravity becomes negligible. For the sake of simplicity, we will refer these particles to as nanoparticles, though particles in micrometer size behave the same and are also included in the discussion here. Furthermore, we will limit our discussion on spherical nanoparticles. Van der Waals force is a weak force and becomes significant only at a very short distance. Brownian motion ensures that nanoparticles are colliding with each other all the time. The combination of van der Waals attraction force and Brownian motion would result in the formation of agglomeration of the nanoparticles.

Van der Waals interaction between two nanoparticles is the sum of the molecular interaction for all pairs of molecules composed of one molecule in each particle, as well as to all pairs of molecules with one molecule in a particle and one in the surrounding medium such as solvent. Integration of all the van der Waals interactions between two molecules over two spherical particles of radius, r, separated by a distance, S. as illustrated in Figure 3.2 gives the total interaction energy or attraction potential as shown in equation (3.2).

$$\Phi_A = -\frac{A}{6}\left[\frac{2r^2}{S^2+4rS}+\frac{2r^2}{S^2+4rS+4r^2}+\ln\left(\frac{S^2+4rS}{S^2+4rS+4r^2}\right)\right] \qquad (3.2)$$

Where the negative sign represents the attraction nature of the interaction between two particles, and A is a positive constant termed the Hamaker constant, which has a magnitude on the order of 10^{-19} to 10^{-20} J, and depends on the polarization properties of the molecules in the two particles and in the medium which separates them. Table 3.2 listed some Hamaker constants for a few common materials. Equation (3.2) can be simplified under various boundary conditions. For example, when the separation distance between two equal sized spherical particles are significantly smaller than the particle radius, i.e. S/r <<1, the simplest expression of the van der Waals attraction could be obtained in equation (3.3).

$$\Phi_A = -\frac{Ar}{12S} \tag{3.3}$$

Other simplified expressions of the van der Waals attraction potential are summarized in Table 3.3. From this table, it is noticed that the van der Waals attraction potential between two particles are different from that between two flat surfaces. Furthermore, it should be noted that the interaction between two molecules are significantly different from that two particles. Van der Waals interaction energy between two molecules can be simply represented by equation (3.4).

$$\Phi_A \alpha - S^{-6} \tag{3.4}$$

Although the nature of attraction energy between two particles is the same as that between two molecules, integration of all the interaction between molecules from two particles and from medium results in a totally different dependence of force on distance. The attraction force between two particles decays much slowly and extends over distances of nanometers. As a result, a barrier potential must be developed to

prevent agglomeration. Two methods are widely applied to prevent agglomeration of particles: electrostatic repulsion and steric exclusion.
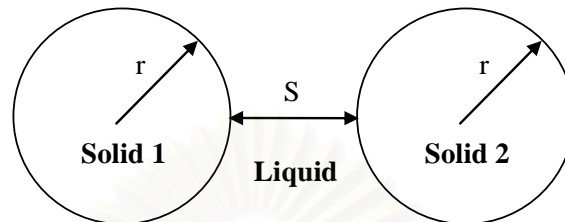
Figure 3.2 Pair of particles used to derive the van der Waals interaction

Table 3.2 Hamaker constants for some common materials

Materials	$A(10^{-20} \text{ J})$
Metal	16.2-45.5
Gold	45.3
Oxides	10.5-15.5
Al_2O_3	15.4
MgO	10.5
SiO_2 (fused)	6.5
SiO_2 (quartz)	8.8
Ionic crystal	6.3-15.3
CaF_2	7.2
Calcite	10.1
Polymers	6.15-6.6
Polyvinyl chloride	10.82
Polyehtylene oxide	7.51
Water	4.35
Acetone	4.20
Carbon tetrachloride	4.78
Chlorobenzene	5.89
Ethyl acetate	4.17
Hexane	4.32
Toluene	5.40

Table 3.3 Simple formulas for van der Waals attraction between two particles

Particles	Φ_A
Two spheres of equal radius, r *	$-Ar/12S$
Two spheres of unequal radii, r_1 and r_2 *	$-Ar_1r_2/6S(r_1+r_2)$
Two parallel plates with thickness of δ, interaction per unit area	$-A/12\pi[S^{-2}+(2\delta+S)^{-2}+(\delta+S)^{-2}]$
Two blocks, interaction per unit area	$-A/12\pi S^2$

* r, r_1 and r_2 >> S

3.2.3 Electrostatic repulsion

There are a variety of mechanisms by which colloidal particles may acquire a net surface charge. Obviously, like-charged surfaces will repel each other and so is an important way of imparting stability to colloids. To understand this situation we must describe the ionic atmosphere, called the electrical double layer, around a charged particle. The theory is based on Coulomb's law to calculate the free energy of repulsion due to the charge, and also Boltzmann's distribution law to calculate how the charge is distributed in the solution. At low salt concentrations the result can be approximated by equation (3.5)

$$\Phi_R = 2\pi\varepsilon_r\varepsilon_0 r\varsigma^2 e^{-\kappa S} \qquad (3.5)$$

where r is radius of two equally sized spherical particles, ε_r is the dielectric constant of the solvent and ε_0 is the permittivity of vacuum. The important result is that the electrical repulsion depends exponentially on the surface separation S

The parameter ς is called the zeta potential of the particles and may be thought of as the electrical potential at the surface of the particles. Typical values are in the range 0 - ±100 mV. The other term κ (dimensions 1/length) is called the reciprocal Debye length, and is a measure of how far the double layer extends from the particle

surface. At 298 K when the electrolyte concentrations are expressed in mol/l, Debye length can be calculated by equation (3.6).

$$\kappa = 3.29\sqrt{I} \qquad nm^{-1} \tag{3.6}$$

where the ionic strength (I) is calculated from the concentrations c_i and valencies z_i of all species of ions in the solution as shown in equation (3.7).

$$I = \frac{1}{2}\sum c_i z_i^2 \tag{3.7}$$

3.2.4 Interactions between two particles: DLVO theory

The total interaction between two particles, which are electrostatic stabilized, is the combination of van der Waals attraction and electrostatic repulsion as shown in equation (3.8).

$$\Phi_{DLVO} = \Phi_A + \Phi_R \tag{3.8}$$

The electrostatic stabilization of particles in a suspension is successfully described by the DLVO theory, named after Derjaguin, Landau, Verwey and Overbeek. The interaction between two particles in a suspension is considered as the combination of van der Waals attraction potential and the electric repulsion potential. There are some important assumptions in the DLVO theory:

1. Infinite flat solid surface

2. Uniform surface charge density

3. No redistribution of surface charge, i.e. the surface electric potential remains constant

4. No change of concentration profiles of both counter ions and surface charge determining ions, i.e. the electric potential remains unchanged

5. Solvent exerts influences via dielectric constant only, i.e. no chemical reactions between the particles and solvent

It is very clear that some of the assumptions are far from the real picture of two particles dispersed in a suspension. For example, the surface of particles is not infinitely flat, and the surface charge density is most likely to change when two charged particles get very close to each other. However, in spite of the assumptions, the DLVO theory works very well in explaining the interactions between two approaching particles, which are electrically charged, and thus is widely accepted in research community of colloidal science.
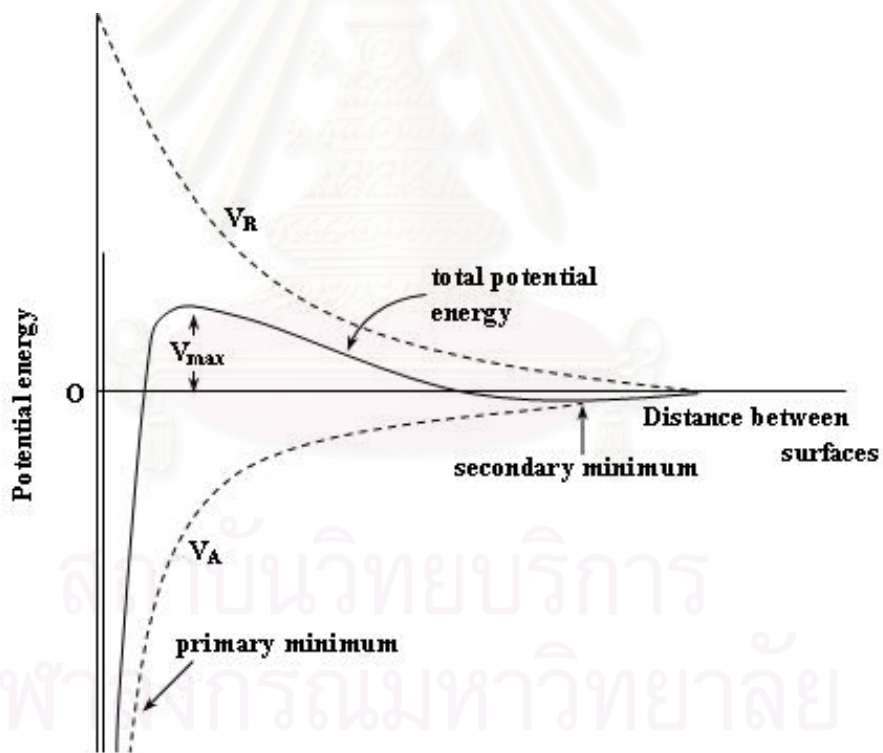

Figure 3.3 Schematic of DLVO potential: V_A= attractive van der Waals potential,

V_R= repulsive electrostatic potential

Figure 3.3 shows the van der Waals attraction potential, electric repulsion potential, and the combination of the two opposite potentials as a function of distance from the surface of a spherical particle. At the distance far from the solid surface, both van der Waals attraction potential and electrostatic repulsion potential reduce to zero. Near the surface is a deep minimum in the potential energy produced by the van der Waals attraction. A maximum is located a little farther away from the surface, as the electric repulsion potential dominates the van der Waals attraction potential. The maximum is also known as repulsive barrier. If the barrier is greater than ~10kT, where k is Boltzmann constant, the collisions of two particles produced by Brownian motion will not overcome the barrier and agglomeration will not occur.

3.3 Optical properties : surface plasmon resonance

The reduction of material's dimension has pronounced effects on the optical properties. The size dependence can be generally classified into two groups. One is due to the increased energy level spacing as the system becomes more confined, and the other is related to surface plasmon resonance.

Surface plasmon resonance is the coherent excitation of all the "free" electrons within conduction band, leading to an in-phase oscillation. When the size of a metal nanocrystal is smaller than the wavelength of incident radiation, a surface plasmon resonance is generated and Figure 3.4 shows schematically how a surface plasmon oscillation of metallic particle is created in a simple manner. The electric filed of an incoming light induces a polarization of the free electron relative to the cationic lattice. The net charge difference occurs at the nanoparticle boundaries (the surface), which in turn acts as a restoring force. In this manner a dipolar oscillation of electron is

created with a certain frequency. The surface plasmon resonance is a dipolar excitation of the entire particle between the negatively charged free electrons and its positively charged lattice. The energy of surface plasmon resonance depends on both the free electron density and the dielectric medium surrounding the nanoparticle. The width of resonace varies with the characteristic time before electron scattering. For larger nanoparticle, the resonance sharpens as the scattering length increases. Noble metal has the resonance frequency in the visible light range.

In small particles, electron surface scattering becomes significant, when the mean free path of conduction electrons is smaller than the physical dimension of the nanoparticles. For example, conduction electrons in silver and gold have a mean free path of 40-50 nm and will be limited by the particle surfaces in particles of 20 nm. If the electrons scatter with the surface elastic but totally random way, the coherence of the overall plasmon oscillation is lost. Inelastic electron-surface collisions would also change the phase. The smaller the particles, the faster the electrons reach the surface of the particles, the electrons can scatter and lose the coherence more quickly. As a results, the plasmon bandwidth increases with decreasing particle size.
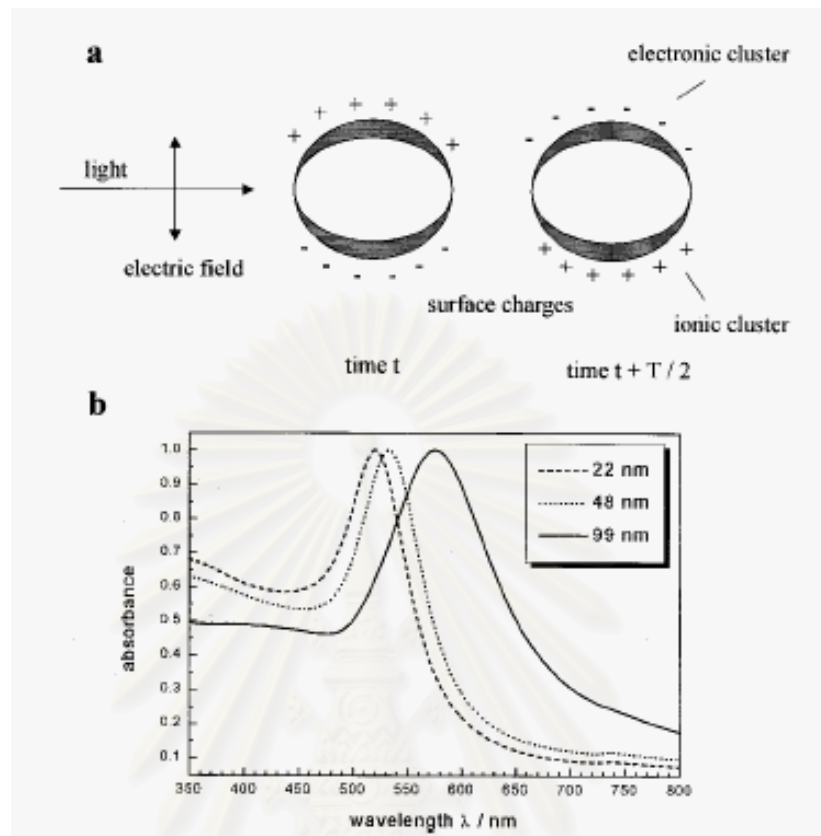
Figure 3.4 Surface plasmon absorption of spherical nanoparticles and its size dependence. (a) A schematic illustrating the excitation of the dipole surface plasmon oscillation. The electric field of an incoming light wave induces a polarization of the (free) conduction electrons with respect to the much heavier ionic core of a spherical gold nanoparticle. A net charge difference is only felt at the nanoparticle boundaries (surface) which in turn acts as a restoring force. In this way a dipolar oscillation of the electrons is created with period T. This is known as the surface plasmon absorption. (b) Optical absorptionspectra of 22, 48 and 99 nm spherical gold nanoparticles. The broad absorption band corresponds to the surface plasmon resonance.

CHAPTER IV

EXPERIMENTAL

4.1 Materials

Gold (III) chloride trihydrate (HAuCl₄.3H₂O), tri-sodium citrate, 2-hydrate (Na₃C₆H₅O₇.2H₂O), hydrochloric acid (HCl) and sodium hydroxide (NaOH) were purchased from Sigma-Aldrich and Kishida as reagent grade. The structures of gold (III) chloride and tri-sodium citrate are shown in Figure. 4.1.
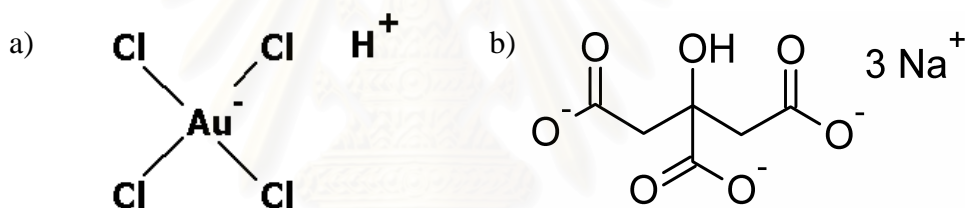
Figure 4.1 Structures of a) gold (III) chloride, b) tri-sodium citrate

4.2 Experimental setup

4.2.1 Experimental apparatus for synthesis of gold nanoparticles

As seen in Figure 4.2, temperature of reacting solution was controlled by a temperature controller attached to a heater. Evaporating vapor was condensed by a condenser and returned to system. Working volume was fixed at 10 ml all batches. An ultrasonic probe was used for applying sonication power to the solution. The end of probe was dipped in solution only 1-2 mm to make sure that sonication power was applied to all solution.

Water out

Water in

5

4

6

3

2 1

1. **Temperature controller**
2. **Thermometer**
3. **Heater**
4. **Condenser**
5. **Ultrasonic probe**
6. **Silicon seal**
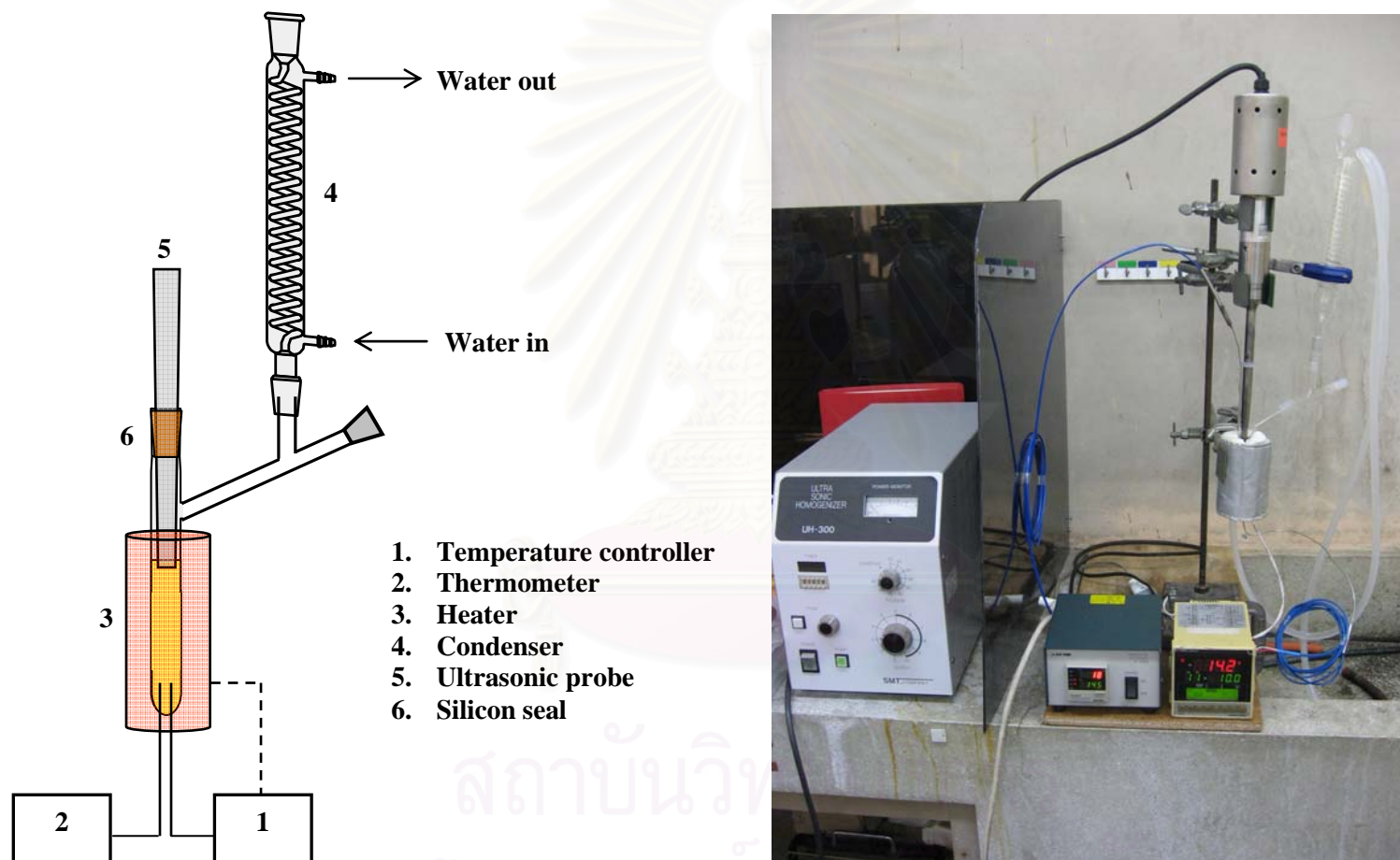
Figure 4.2 Experimental apparatus for synthesis of gold nanoparticles

4.2.2 Experimental apparatus for testing ozone sensor

A diagram of this apparatus was shown in Figure 4.3. Oxygen was separated into two lines. The first line passed through ozone generator for making ozone while the other was used for supplying water vapor by bubbling method to sensor for eliminating an effect of humidity. The humidity was always fixed at 95.6%. Sensor was directly connected to a multi-meter for transferring data to computer. After measurement, all gas was passed through activated carbon column for safety. Drawing and photos of sensor were shown in Figure 4.4.
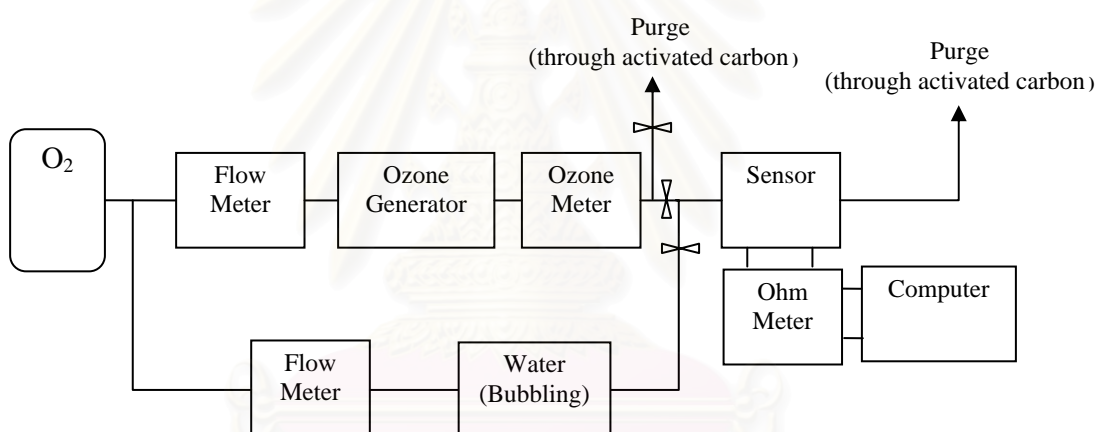
Figure 4.3 Experimental apparatus to evaluate sensors for detecting ozone gas
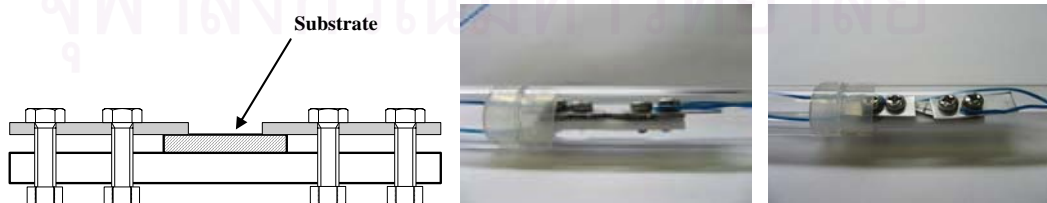
Figure 4.4 Drawing and Photos of sensor

To compare sensitivity to ozone gas, three kinds of sensor were investigated. They consisted of carbon nanotubes (CNTs) sensor, gold nanoparticles sensor and CNTs-gold nanoparticles sensor. Firstly, CNTs-sensor, CNTs film was synthesized by the CVD method on silicon wafer (Appendix A1). The width and thickness of synthesized CNTs film was 1 mm and 30 μm, respectively. SEM images of CNTs film on silicon wafer was shown in Figure 4.5. For gold nanoparticles sensor, Pt was coated on silicon wafer as shown in Figure 4.6. A narrow space between both coated areas was 1 mm. Next, we dropped gold nanoparticles solution (average diameter of gold nanoparticles was 16 nm) for connecting both area and dried in the oven for 1 hour.
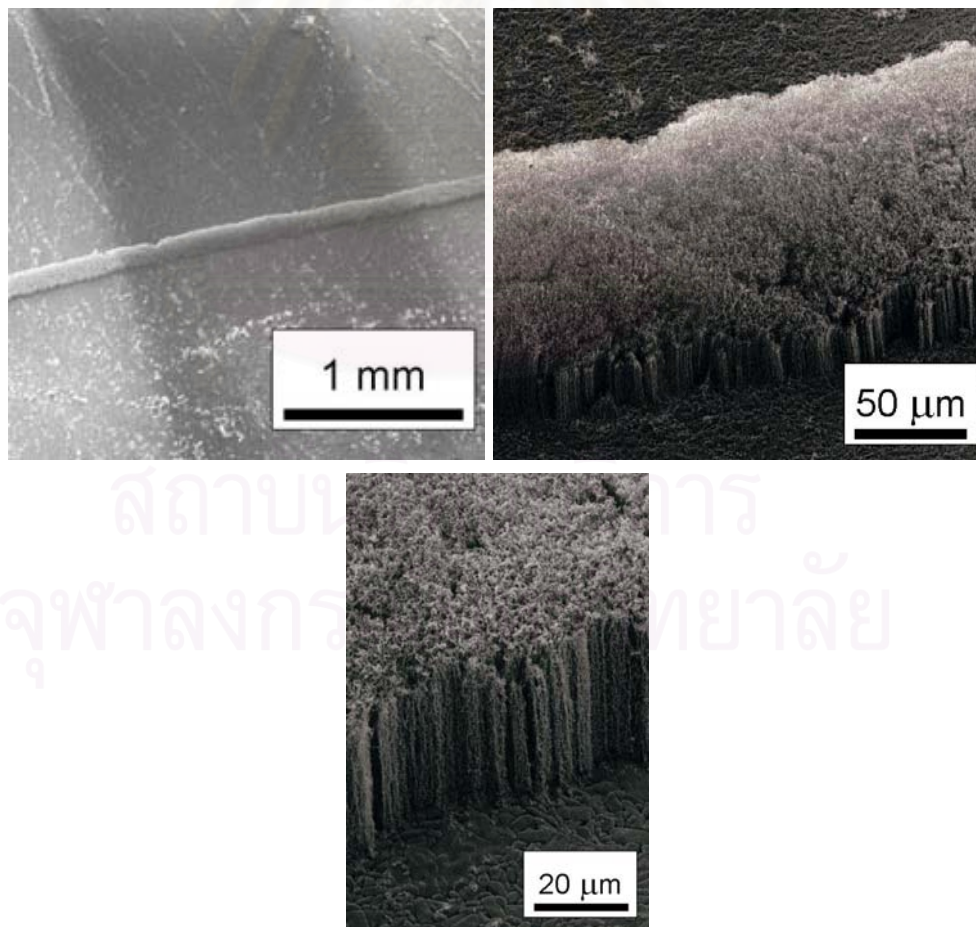
Figure 4.5 SEM images of CNTs film on silicon wafer
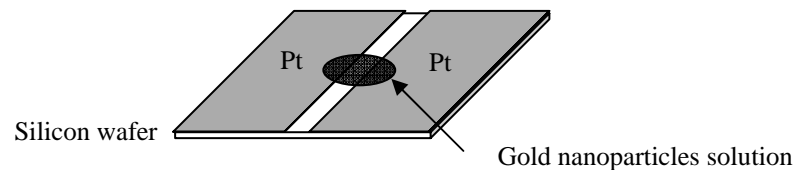
Figure 4.6 Gold nanoparticles sensor

For CNTs-gold nanoparticles sensor, CNTs film was synthesized by the CVD method described in Appendix A1. Next, silicon wafer substrate was treated by H_2O_2 about an hour until CNTs was able to absorb water (Normally, CNTs film was hydrophobic). Afterwards, substrate was sunk in gold nanoparticles solution (average diameter of gold nanoparticles was 16 nm) about 18 hours. For making sure that gold nanoparticles attached on CNTs surface, CNTs film, which treated by this method, was analyzed by TEM. TEM images of CNTs attached by gold nanoparticles were shown in Figure 4.7 and Figure 4.8. From Figure 4.8, this evidence proved that gold nanoparticles were really attached on the CNTs surface.
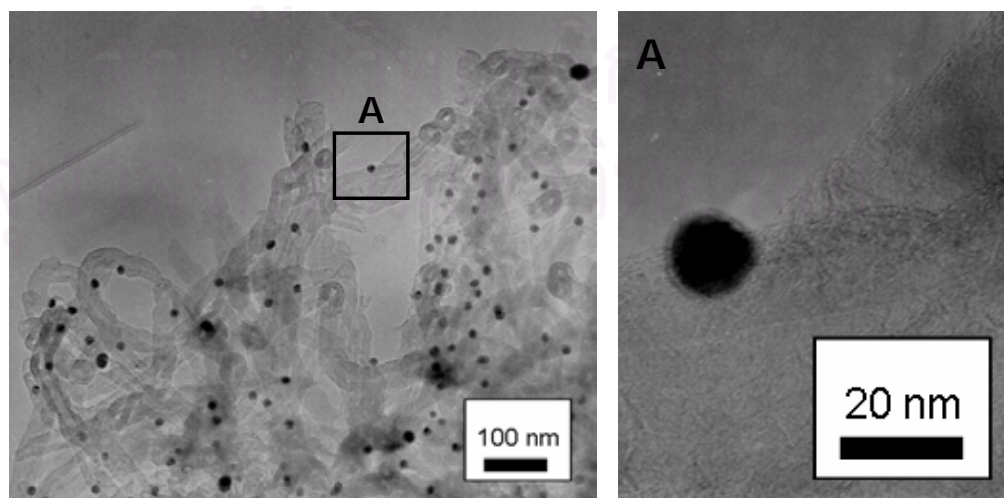
Figure 4.7 TEM images of CNTs attached by gold nanoparticles
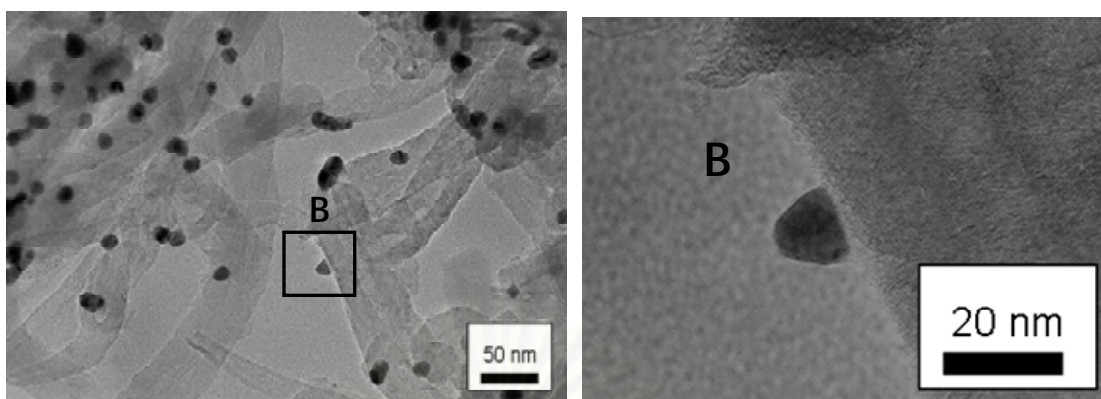
Figure 4.8 TEM images of gold nanoparticles on CNTs surface

4.3 Experimental procedures

4.3.1 Molar ratio of precursor to reducing agent

According to literature review in chapter II, sizes of gold nanoparticles strongly depended on molar ratio of precursor to reducing agent. Anyway, this parameter was still investigated under the conditions given in Table 4.1. This result will be used for comparing with other paper and used as standard gold solution to make a sensor. All conditions were run at boiling temperature of the solution (approximately 100 ^{O}C) for 10 minutes.

Table 4.1 Experimental conditions for preparing gold nanoparticles at various molar ratios between gold (III) chloride and tri-sodium citrate

Condition No.	Gold (III) chloride solution		Tri-sodium citrate solution		Distilled water	Total conc.	Molar ratio
	Volume (cm^3)	Conc. (mol/dm^3)	Volume (cm^3)	Conc. (mol/dm^3)	Volume (cm^3)	(mol/dm^3)	
1	1.0	2.03×10^{-2}	1.0	2.03×10^{-2}	8.0	0.41×10^{-2}	1:1
2	1.0	2.03×10^{-2}	1.0	4.06×10^{-2}	8.0	0.61×10^{-2}	1:2
3	1.0	2.03×10^{-2}	1.0	10.16×10^{-2}	8.0	1.22×10^{-2}	1:5
4	1.0	2.03×10^{-2}	1.0	20.32×10^{-2}	8.0	2.24×10^{-2}	1:10
5	1.0	2.03×10^{-2}	1.0	30.48×10^{-2}	8.0	3.25×10^{-2}	1:15
6	1.0	2.03×10^{-2}	1.0	40.64×10^{-2}	8.0	4.27×10^{-2}	1:20

4.3.2 Total concentration of reactants

For investigating effect of total concentration of reactants, gold (III) chloride and tri-sodium citrate solution was prepared as shown in Table 4.2. Molar ratio was equal to 1:5 every condition. Every batch was run at boiling temperature of the solution.

Table 4.2 Experimental conditions for preparing gold nanoparticles at various total concentrations of gold (III) chloride and tri-sodium citrate

Condition No.	Gold (III) chloride solution		Tri-sodium citrate solution		Distilled water	Total Concentration
	Volume (cm^3)	Conc. (mol/dm^3)	Volume (cm^3)	Conc. (mol/dm^3)	Volume (cm^3)	(mol/dm^3)
7	1.0	0.51×10^{-2}	1.0	2.54×10^{-2}	8.0	0.31×10^{-2}
8	1.0	2.54×10^{-2}	1.0	12.70×10^{-2}	8.0	1.52×10^{-2}
9	1.0	12.70×10^{-2}	1.0	63.50×10^{-2}	8.0	7.63×10^{-2}

4.3.3 Reaction temperature

For investigating effect of reaction temperature, the temperatures were tested at 60 ^{O}C, 80 ^{O}C, and boiling temperature (approximately 100 ^{O}C). Molar ratio was also equal to 1:5 every condition.

4.3.4 Sonication power

After making calibration graph for sonication machine (Appendix A2), the sonication powers were carried at 0, 7.6, 15.2, 22.8, and 30.5 W. All conditions are run at boiling temperature of the solution for 10 minutes. Molar ratio was kept constant at 1:5 every condition.

4.3.5 *pH* of precursors

The pH of the gold nanoparticle solution was adjusted by varying hydrochloric acid (HCl) or sodium hydroxide solution (NaOH) concentration as shown in Table 4.3 and Table 4.4. All conditions were run at boiling temperature of the solution for 10 minutes. Molar ratio is also equal to 1:5.

Table 4.3 Experimental conditions for investigating effect of pH in range of 3.1-6.2

Condition No.	Gold (III) chloride solution		Tri-sodium citrate solution		Hydrochloric acid		Distilled water	pH
	Volume (cm^3)	Conc. (mol/dm^3)	Volume (cm^3)	Conc. (mol/dm^3)	Volume (cm^3)	Conc. (mol/dm^3)	Volume (cm^3)	
10	1.0	2.03×10^{-2}	1.0	10.16×10^{-2}	-	-	8.0	6.2
11	1.0	2.03×10^{-2}	1.0	10.16×10^{-2}	1.0	2.5×10^{-3}	7.0	5.9
12	1.0	2.03×10^{-2}	1.0	10.16×10^{-2}	1.0	1.0×10^{-2}	7.0	5.0
13	1.0	2.03×10^{-2}	1.0	10.16×10^{-2}	1.0	2.0×10^{-2}	7.0	3.9
14	1.0	2.03×10^{-2}	1.0	10.16×10^{-2}	1.0	3.0×10^{-2}	7.0	3.4
15	1.0	2.03×10^{-2}	1.0	10.16×10^{-2}	1.0	4.0×10^{-2}	7.0	3.1

Table 4.4 Experimental conditions for investigating effect of pH in range of 6.2-10.1

Condition No.	Gold (III) chloride solution		Tri-sodium citrate solution		Sodium hydroxide solution		Distilled water	pH
	Volume (cm^3)	Conc. (mol/dm^3)	Volume (cm^3)	Conc. (mol/dm^3)	Volume (cm^3)	Conc. (mol/dm^3)	Volume (cm^3)	
10	1.0	2.03×10^{-2}	1.0	10.16×10^{-2}	-	-	8.0	6.2
16	1.0	2.03×10^{-2}	1.0	10.16×10^{-2}	1.0	5×10^{-3}	7.0	6.8
17	1.0	2.03×10^{-2}	1.0	10.16×10^{-2}	1.0	1.0×10^{-2}	7.0	7.2
18	1.0	2.03×10^{-2}	1.0	10.16×10^{-2}	1.0	1.5×10^{-2}	7.0	9.1
19	1.0	2.03×10^{-2}	1.0	10.16×10^{-2}	1.0	2.0×10^{-2}	7.0	9.8
20	1.0	2.03×10^{-2}	1.0	10.16×10^{-2}	1.0	2.5×10^{-2}	7.0	10.1

4.3.6 Comparing sensitivity to ozone gas among CNTs sensor, gold nanoparticles sensor and CNTs-gold nanoparticles sensor

From Figure 4.3, oxygen was supplied to a sensor cell at flow rate = 1 L/min and waited until the resistance of sensor seems stable (about 1-2 hour). Next, we started to record these data for 5 minutes. Afterwards, the other line, ozone was supplied to a sensor at the same flow rate (concentration of ozone was 20 g/m^3, the total flow rate is equal to 2 L/min) and recorded the changing of resistance for 10

minutes. Lastly, we switched off the ozone line and recorded the resistance for another 5 minutes.

4.4   Analytical instruments

Ultraviolet and visible (UV-Vis) spectra emitted from prepared suspension were detected at room temperature using a UV-visible spectrophotometer (Shimadzu, UV-1600PC). The particle size distribution and zeta potential of the gold nanoparticles were measured using a dynamic light scattering (Malvern, Zetasizer 3000 HS$_A$). Size and morphology of gold nanoparticles were studied by Transmission Electron Microscope (TEM) (JEOL, JEM-3010)

CHAPTER V

RESULTS AND DISCUSSION

5.1 Effect of molar ratio of precursor to reducing agent

Based on our experimental results, gold colloids synthesized under conditions of higher molar ratio of sodium citrate (1:5 to 1:20) exhibited a clear red color while conditions of lower reducing agent molar ratio (1:1 and 1:2) provided turbid red-purple suspensions (Figure 5.1). With UV-vis spectrophotometric analyses also shown in Figure 5.1, it was found that each product possessed different Maximum Absorption Wavelength (MAW) suggesting that the synthesized gold nanoparticles had different particle sizes (Cao, 2004). Under the condition of 1:5 molar ratio, gold nanoparticles at the lowest MAW (519 nm) were obtained. This result suggested that the possibly smallest gold nanoparticles (d_p ~16 nm) could be synthesized.

Particle size distributions and analytical results based on DLS analyses are summarized in Figure 5.2 and Table 5.1, revealing that size of gold nanoparticles synthesized in this work is in a range of 16-45 nm. DLS results are in a good agreement with the particle size estimated from MAW. It could be confirmed that the smallest particles were prepared under the condition of 1:5 molar ratio of $HAuCl_4$ to $Na_3C_6H_5O_7$. Figure 5.3 reveals a typical TEM image of products synthesized under such condition, which posses the uniform size of approximate 16 nm. Standard deviation of DLS diameter of gold nanoparticles reveals that they posses the very narrow size distribution at the higher molar ratio. Under the conditions of lower molar

ratio (1:1 or 1:2), the electron donor, sodium citrate, would not be sufficient to react with $HAuCl_4$, resulting in an agglomeration of synthesized gold nanoparticles owing to the van der waal interaction (Turkevitch et al., 1951; Fren, 1973). Calculated results of Rayleigh diameter from MAW are also included in Table 5.1. With comparison of DLS and Rayleigh analyses, the minimum diameter could be obtained under the same condition of molar ratio 1:5.
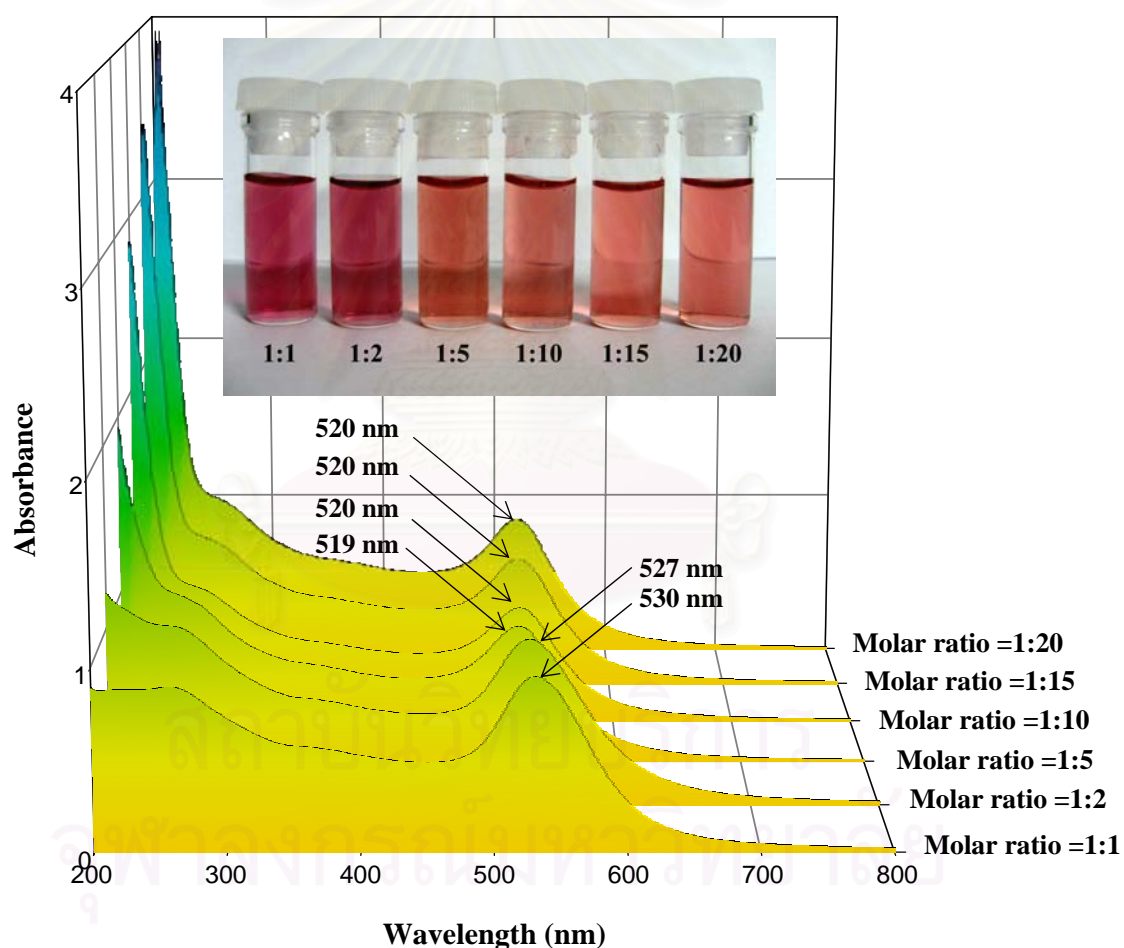

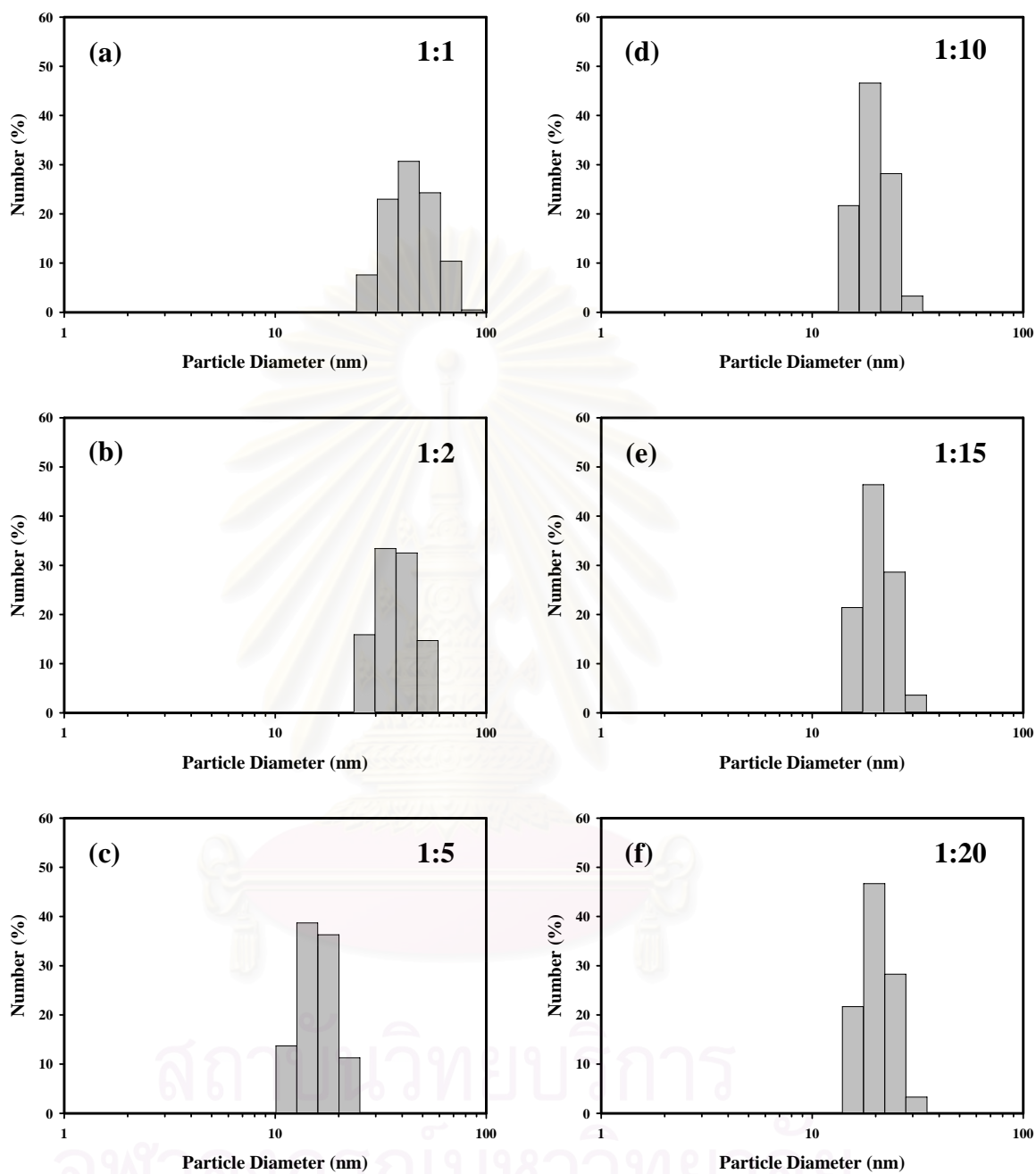**Figure 5.1** UV-vis spectra of gold colloids synthesized in various molar ratios

Figure 5.2 Particle size distributions of gold nanoparticles synthesized in various
molar ratios of $HAuCl_4$ to $Na_3C_6H_5O_7$ (a) 1:1, (b) 1:2, (c) 1:5, (d) 1:10, (e) 1:15, and
(f) 1:20

On the other hand, with the increased molar ratio of $Na_3C_6H_5O_7$ the excessive reducing agents would be adsorbed on the surface of synthesized gold nanoparticles, resulting in a decrease in the surface charge of the nanoparticles, which causes the reversible coagulation of the nanoparticles (Chow, Zukoski, and Grieser, 1993). The evidence of excessive sodium citrate could be noticed from the UV-absorbance at the wavelength of 200 nm as shown in Figure 5.1. As a result, it could be found that the smallest gold nanoparticles with a DLS diameter of 16 nm could be controllably synthesized by adjusting the molar ratio of $HAuCl_4$ to $Na_3C_6H_5O_7$.

Table 5.1 Average diameter of synthesized gold colloids prepared in various molar ratios

Molar ratio	Rayleigh diameter D_R (nm)	DLS analysis (nm)	
		D_P (nm)	σ
1:1	25.2	45	11
1:2	25.0	37	7
1:5	24.7	16	3
1:10	24.8	20	4
1:15	24.8	21	4
1:20	24.8	21	4

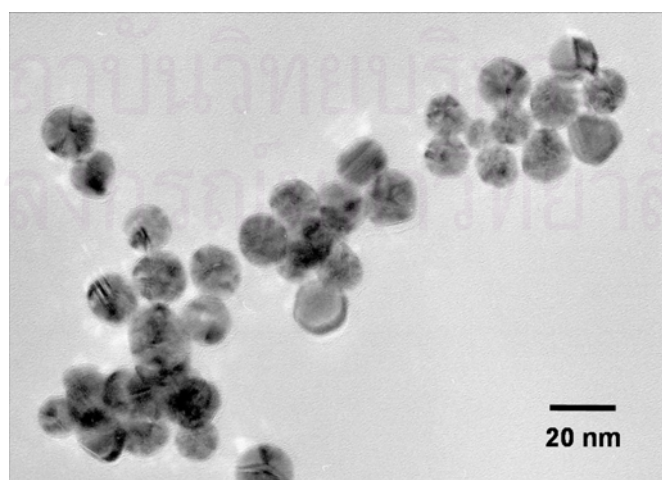**Figure 5.3** Typical TEM image of gold nanoparticles synthesized under condition of 1:5 molar ratio of $HAuCl_4$ to $Na_3C_6H_5O_7$

5.2 Effect of total concentration of reactants

Based on UV-vis spectrophotometric analyses shown in Figure 5.4, an increase in total concentrations of reactants resulted in a shift of MAW to longer wavelength. Table 5.2 showed that reaction time was noticeably faster under condition of higher total concentration. The rate of reaction in the research was determined by photograph evidences as shown in Figure 5.5. This result would be attributed to the collision of particles within the system. An increase in the amount of gold particles synthesized in the system causes the increasing rate of collision, leading to the agglomeration of the particles in the system.
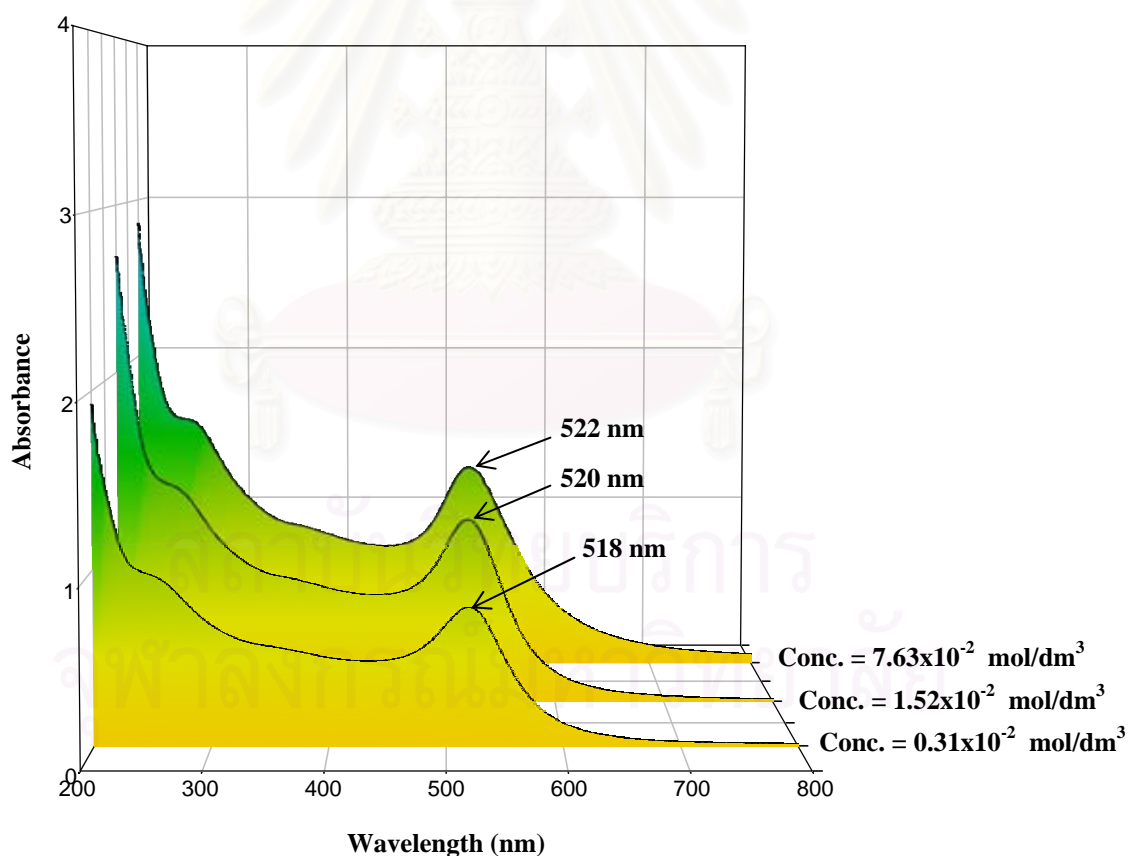

Figure 5.4 UV-vis spectra of gold colloids synthesized under different total

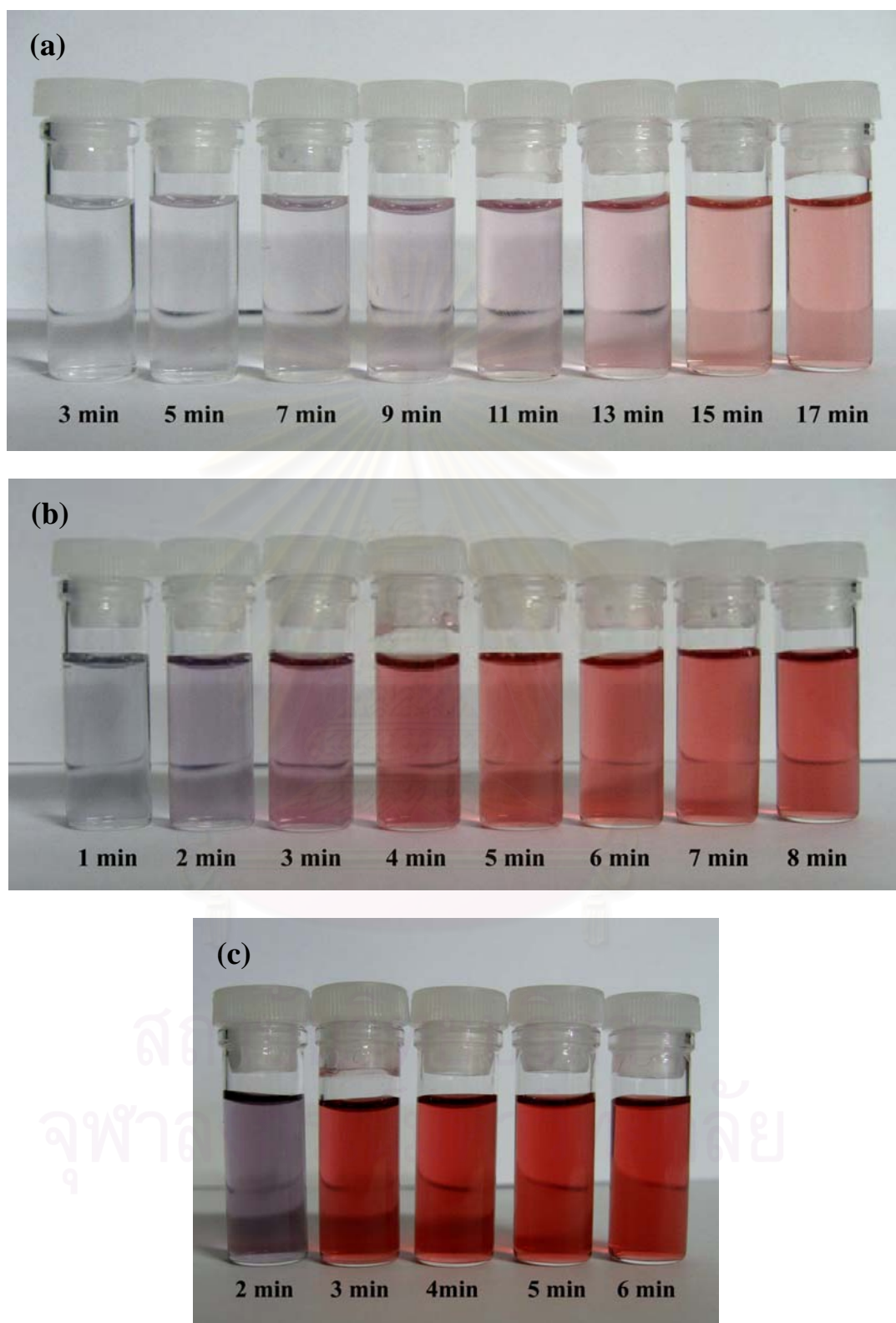concentration of reactants

Figure 5.5 Photograph of gold colloids synthesized under different total concentration

of reactants (a) 0.31×10^{-2} mol/dm^3, (b) 1.52×10^{-2} mol/dm^3 and (c) 7.63×10^{-2} mol/dm^3

Table 5.2 Reaction time of gold colloids prepared under different total concentration

of reactants

Total concentration of reactants (mol/dm^3)	Reaction time (min)
0.31x10^{-2}	15
1.52x10^{-2}	5
7.63x10^{-2}	3

5.3 Effect of reaction temperature

With UV-vis spectrophotometric analyses depicted in Figure 5.6, an increase in

reaction temperature caused a shift of MAW to shorter wavelength. Similar to Table

5.2, Table 5.3 revealed that reaction time was much shorter under condition of higher

reaction temperature. The rate of reaction was qualitatively assessed by photograph

evidences as shown in Figure 5.7. Based on experimental results, it is possible that a

decrease in reaction temperature results in larger size of gold nanoparticles because

the concentration of synthesized gold nanoparticles in suspension exceeds its

equilibrium solubility. The overall energy of the system would be reduced by

segregating gold nanoparticles from the solution (forming a solid phase) (Cao, 2004).

Other possibility to explain this phenomenon is the lower viscosity of solvent by

increasing temperature. Density of solvent also decreases as well. With our

experiment, the temperature increases from 60 ^{O}C to 80°C and 100 ^{O}C. Assume that

the solvent is pure water. Density of solvent will change from 983.200 kg/m^3 to

971.799 kg/m^3 and 958.365 kg/m^3, respectively (Perry's Chemical Engineering

Handbook). 1.2% of solvent volume will change with an increase of temperature from

60 ^{O}C to 80 ^{O}C and another 1.4% of volume will change with an increase of

temperature from 80 ^{O}C to 100 ^{O}C. In nano-scale, the change of volume will

significantly affect on the collision of particles in the system. With the larger volume, a number of collisions among particles will decrease, resulting in smaller obtained size of nanoparticles.
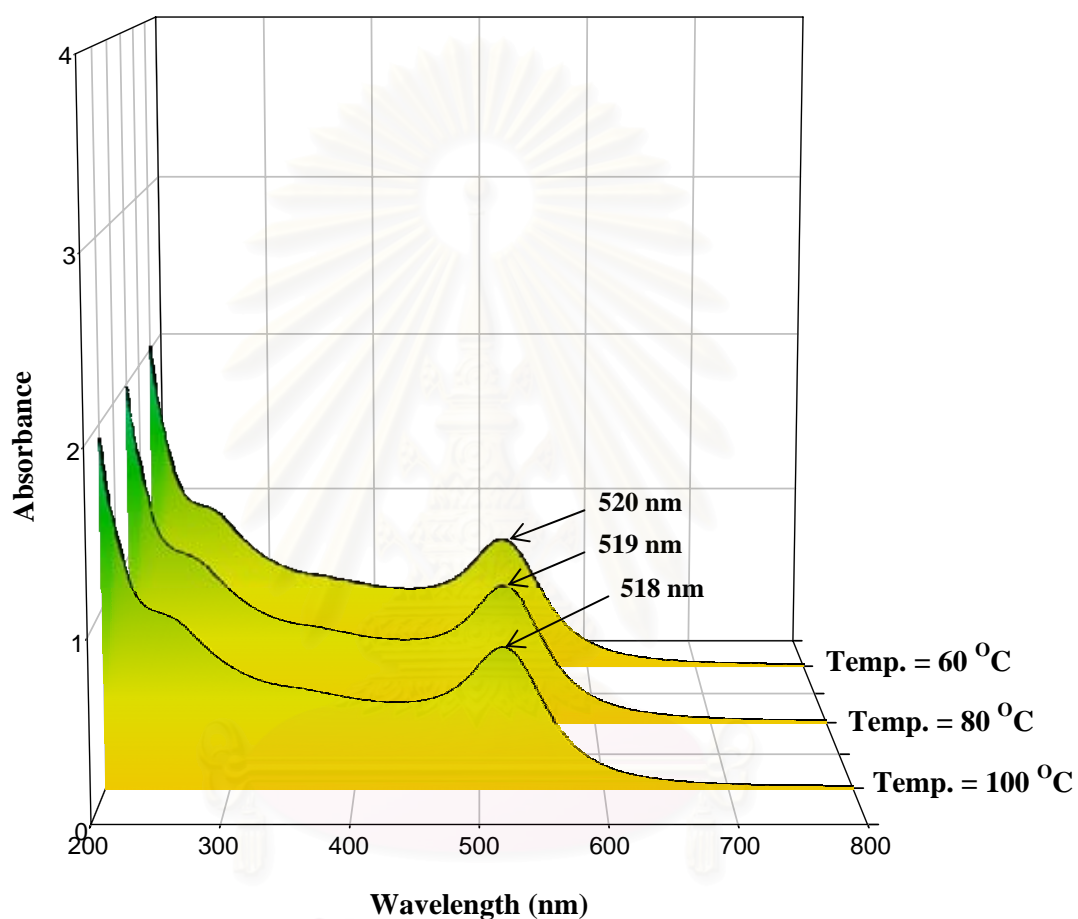

Figure 5.6 UV-vis spectra of gold colloids synthesized under different reaction temperatures

Table 5.3 Reaction time of gold colloids synthesized under different reaction temperatures

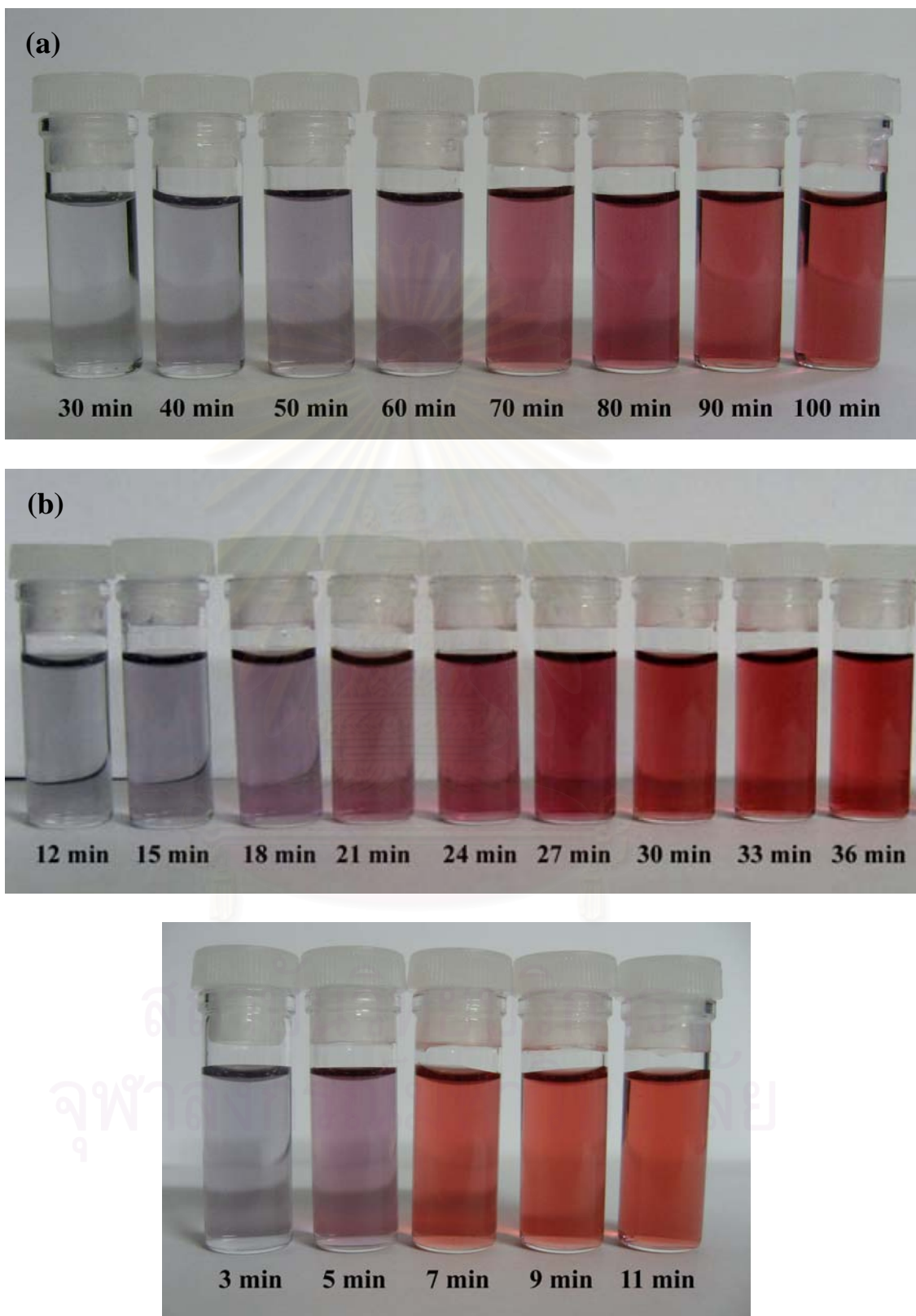| Reaction temperature (^{O}C)	Reaction time (min)
60	90
80	30
100	7

Figure 5.7 Photograph of gold colloids synthesized under different reaction

temperatures (a) 60 ^{O}C, (b) 80 ^{O}C and (c) 100 ^{O}C

5.4   Effect of sonication power

Based on UV-vis spectrophotometric analyses shown in Figure 5.8, it is found that sonication power insignificantly affected on MAW of synthesized products. TEM image shown in Figure 5.9 also confirmed that the size of synthesized gold nanoparticles is around 15-20 nm similar to non-treated solution in Figure 5.3. According to my literature review, Atobe et al. claimed that sonication power strongly affected on the size and shape of gold nanoparticle (Atobe et al., 2005) as shown in Figure 5.10.
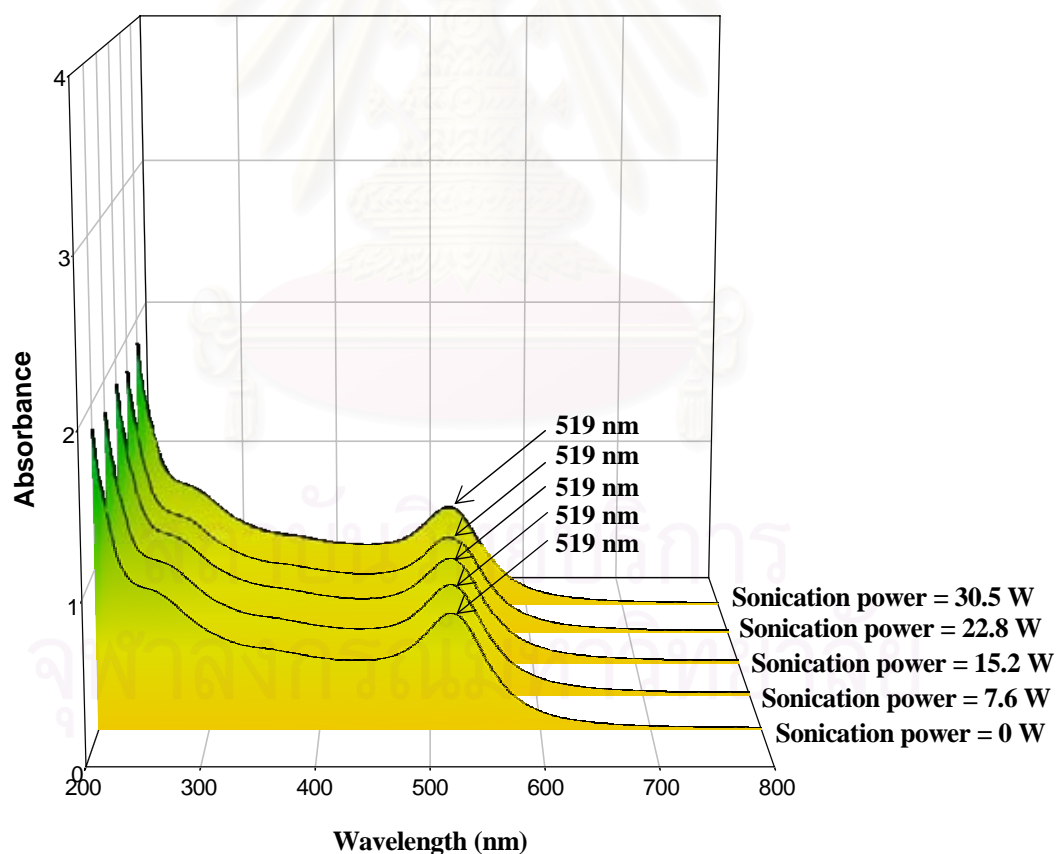

Figure 5.8 UV-vis spectra of gold colloids synthesized under different sonication

power

Based on Atobe et al.'s calculation, they determined the sonication power by adiabatic measurement of the temperature rise of sonicated water. It may be possible to claim that reaction temperature of their experiment increases when they applied sonication power. For that reason, the phenomenon of their experiment may be the same as the case of reaction temperature rising.
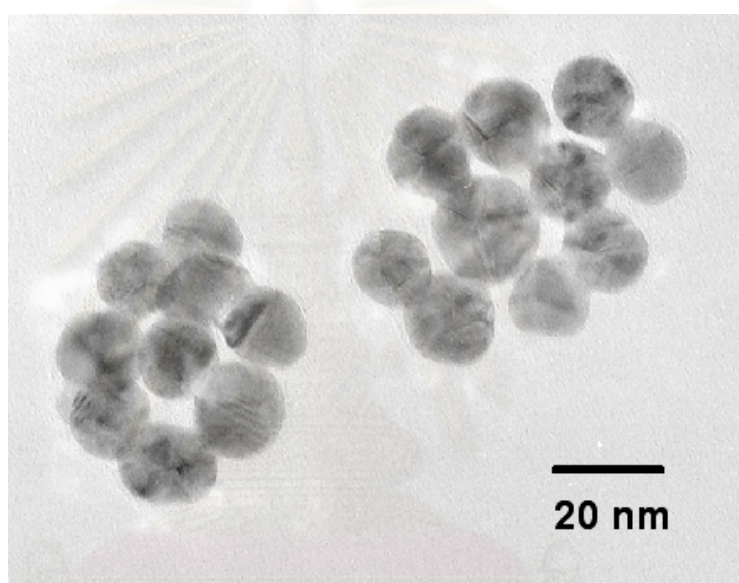

Figure 5.9 TEM image of gold nanoparticles synthesized under sonication power of 30.5 W
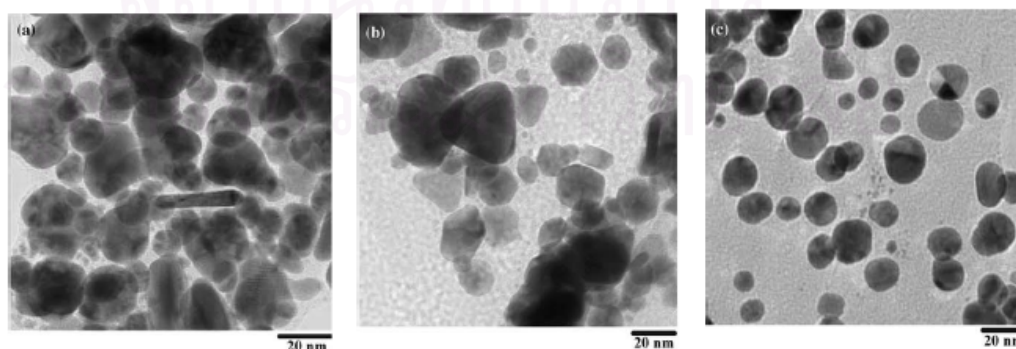

Figure 5.10 TEM images of gold nanoparticles prepared under different sonication power (Atobe et al.): (a) 30 W, (b) 55 W, and (c) 90 W

5.5 Effect of pH

The pH of the gold colloid was adjusted by varying hydrochloric acid (HCl) or sodium hydroxide solution (NaOH). In Figure 5.11, the relationship between pH and zeta potential is depicted. The zeta potentials directly vary to pH of solution. This phenomenon is attributable to the adsorption of the OH^- and H^+ ions on the surface of gold nanoparticles and then the particle surface charge density is changed. The pH and absorption spectra of each gold colloid were measured after the synthesis within 2 hours, showing in Figure 5.12 and Figure 5.13. Photograph of synthesized gold colloids are shown in Figure 5.14.
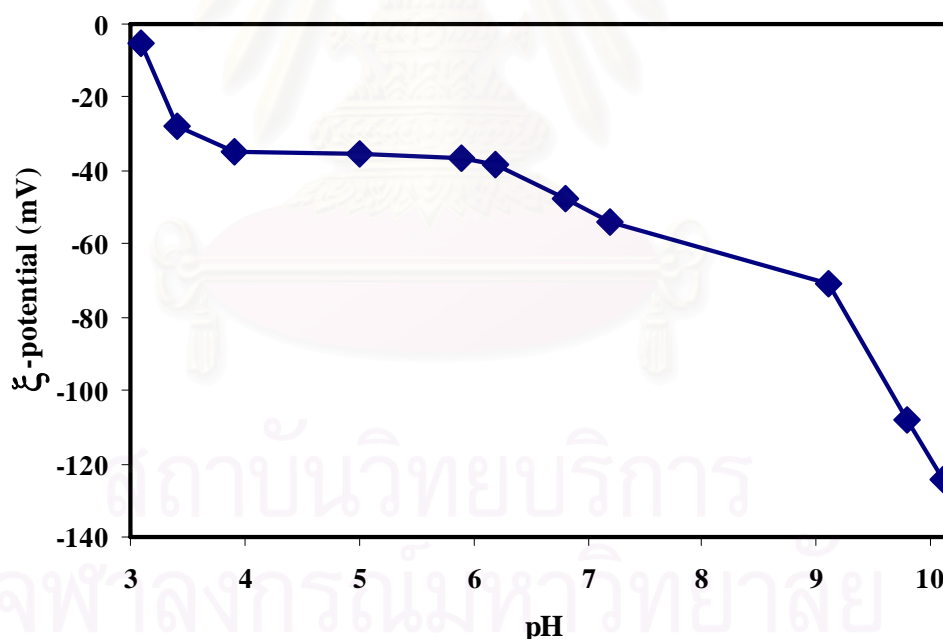

Figure 5.11 A relationship between pH and ξ -potential
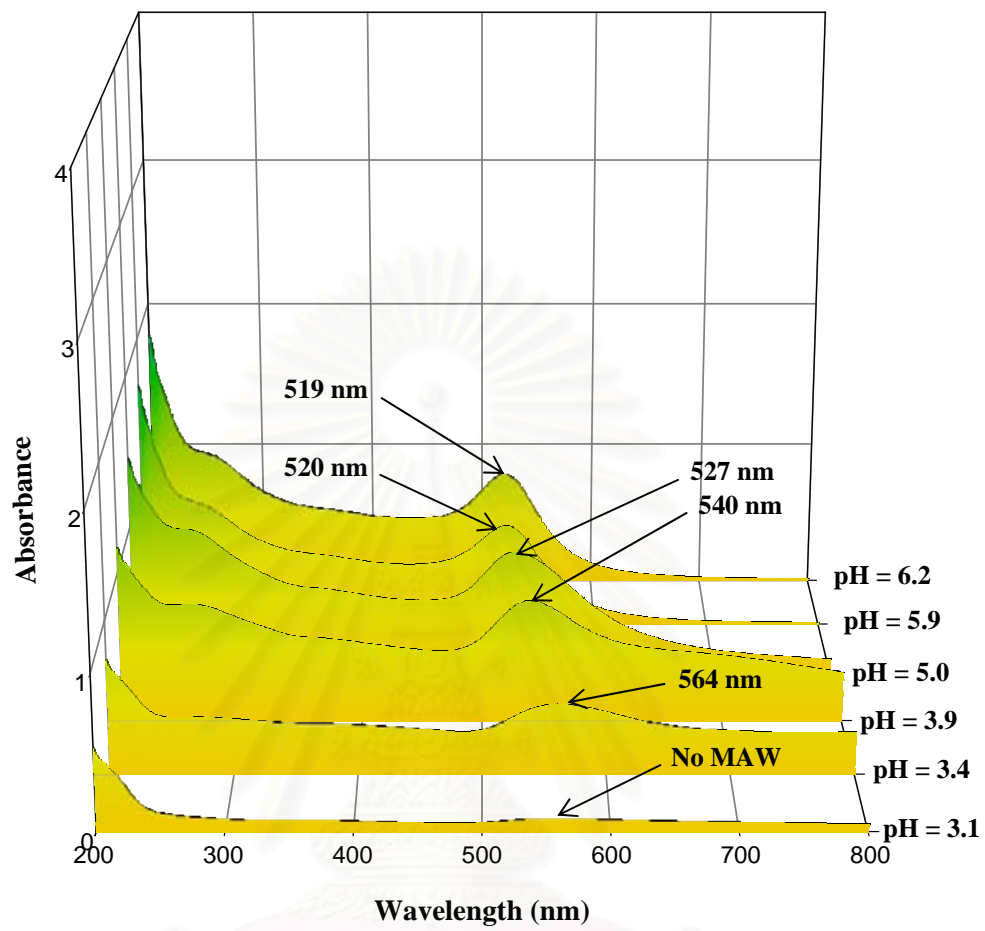
Figure 5.12 UV-vis spectra of gold colloids synthesized when pH of solution is in a range of 3.1-6.2

สถาบันวิทยบริการ

จุฬาลงกรณ์มหาวิทยาลัย
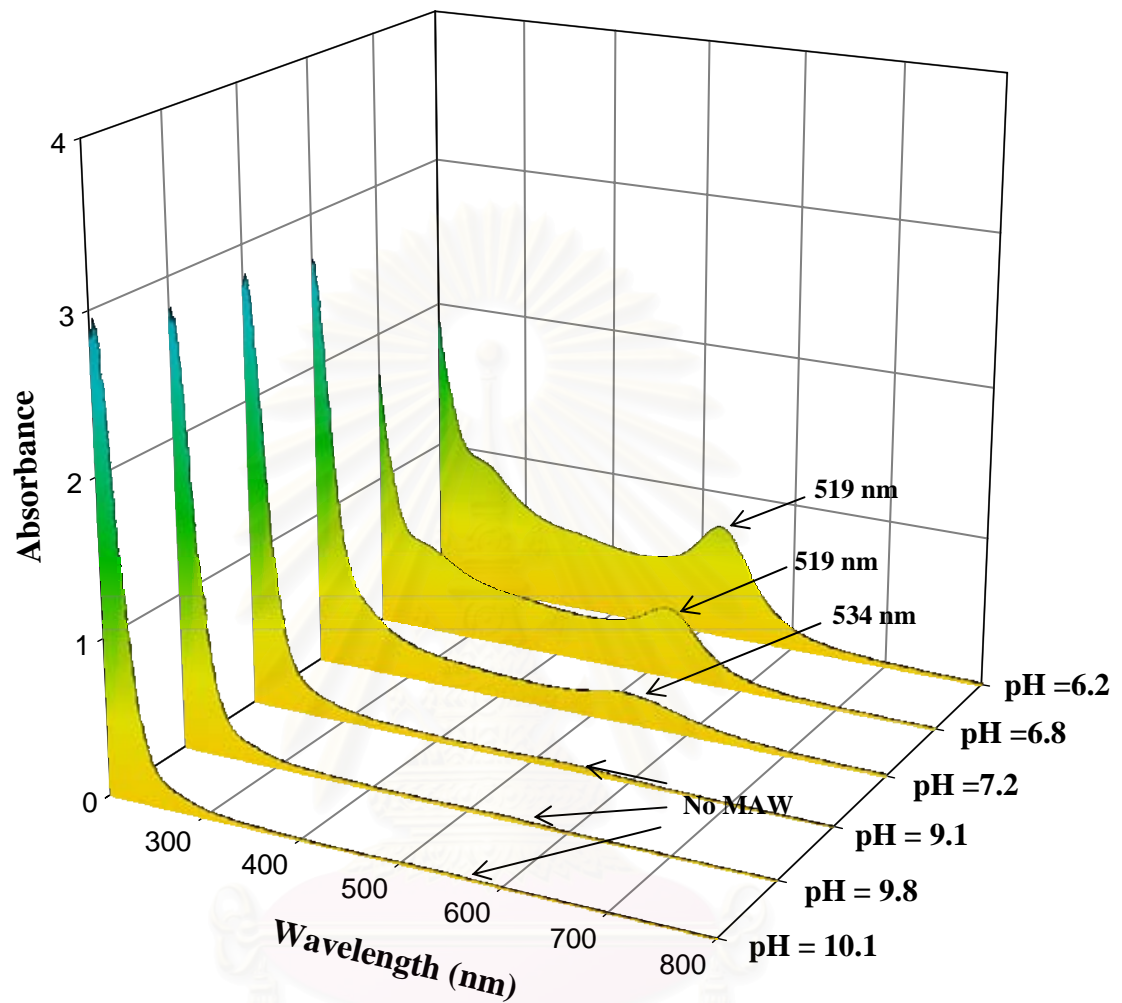
Figure 5.13 UV-vis spectra of gold colloids synthesized when pH of solution is in a range of 6.2-10.1
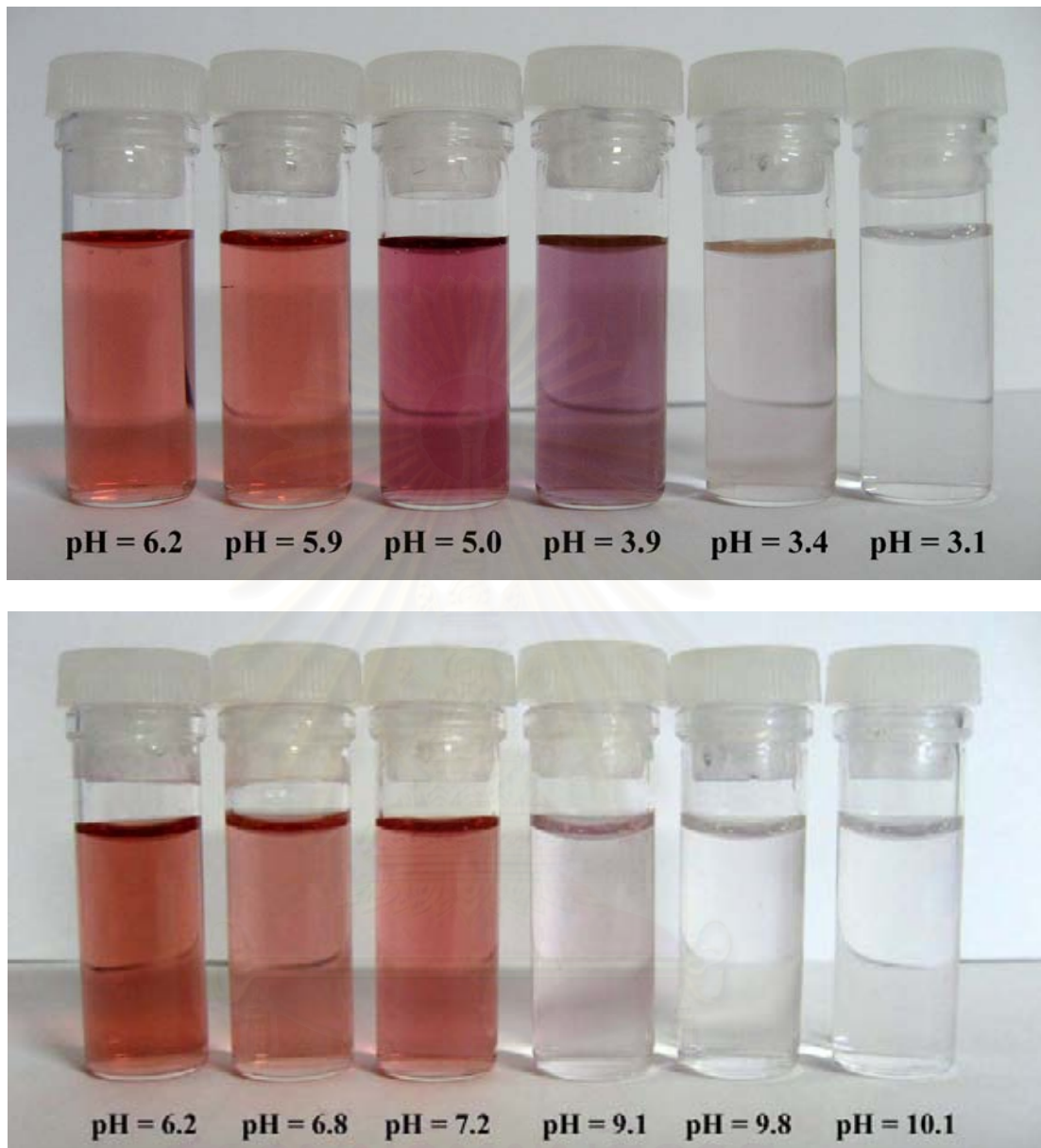
Figure 5.14 Photograph of gold colloids synthesized under different pH of solution

As seen in Figures 5.15-5.17, there are 3 patterns of time dependence of MAW. In the first pattern, when pH is lower than 5.0, the stability of suspension becomes the worse. It could be clearly observed from experiments that suspending particles settle down to the bottom of vessel after leaving for a certain time period. Particles tend to agglomerate faster than non-treated solution (pH is 6.2). In the second scenario, when

pH is in a range of 5.9-7.2, the prepared suspension exhibit very high stability. For such condition, the UV-visible absorbance of suspension is constant for a long time. This is attributed to good dispension of gold nanoparticles which could maintain their electrical potential for a long time without agglomeration (Toshima, Shiraishi, and Arakawa, 2002). In the last situation, when pH is higher than 9.1, gold nanoparticles could be gradually generated, leading to a gradual increase in UV-visible absorption of the suspension. However, the UV-visible absorbance at MAW of the suspension with pH>9.1 became stable after leaving for 2 weeks.
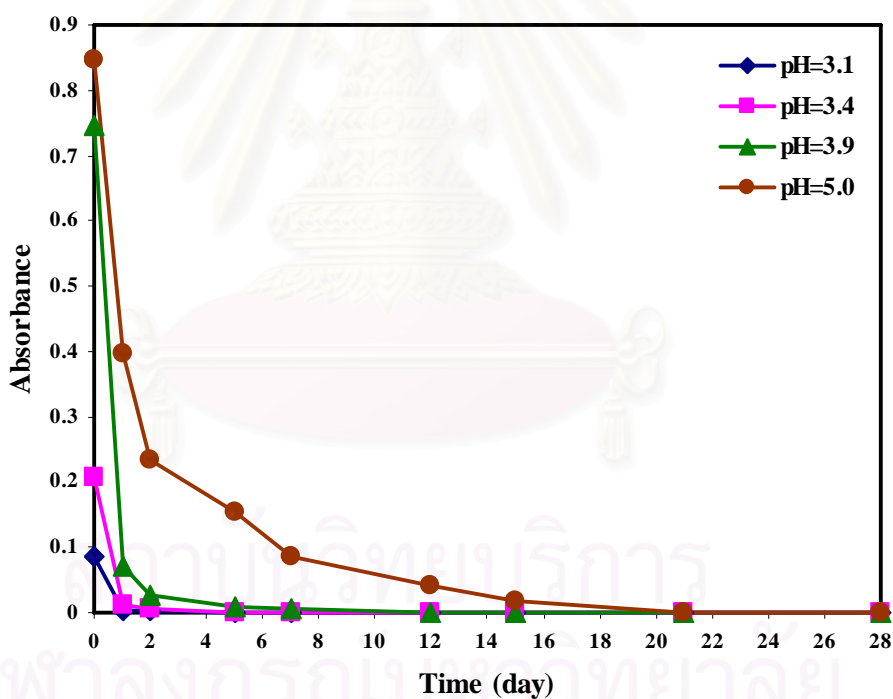

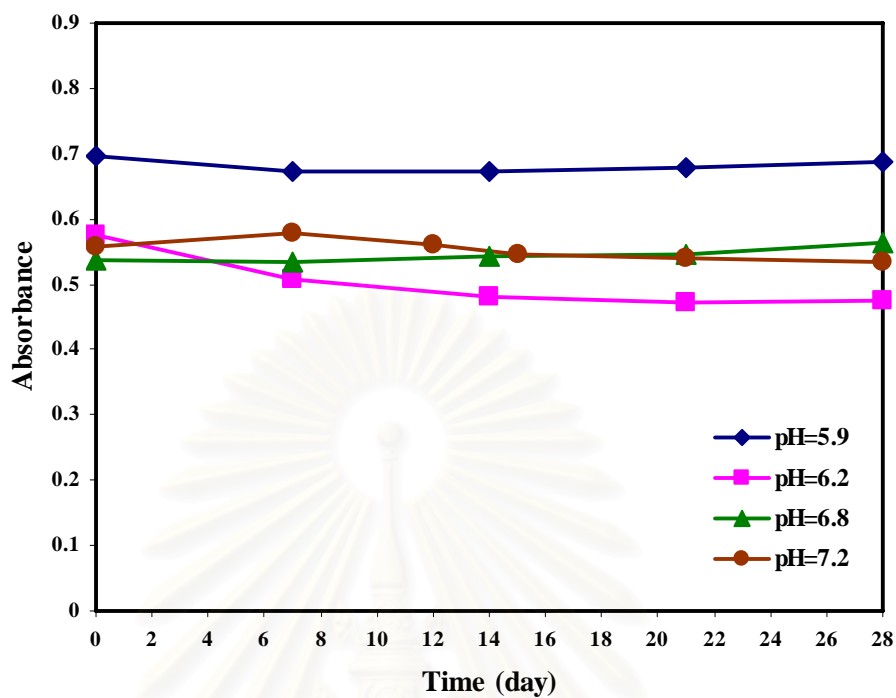**Figure 5.15** Time dependence of UV-visible absorbance at MAW with pH lower than 5.0

Figure 5.16 Time dependence of UV-visible absorbance at MAW with 5.9<pH<7.2
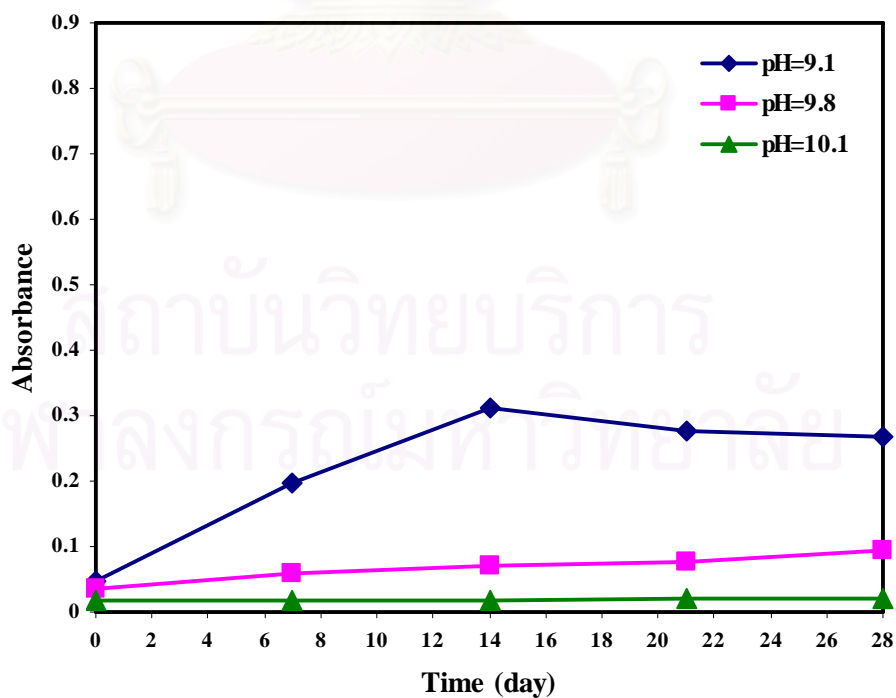

Figure 5.17 Time dependence of UV-visible absorbance at MAW with pH higher

than 9.1

From these results, we can conclude that the rate of agglomeration will be faster if the pH is lower. A possible phenomenon of gold nanoparticle formation can be postulated as shown in Figure 5.18. For the case when pH is below 5.0 with the zeta potential higher than -40 mV, a lot of added hydrogen ions in the solution could be adsorbed on gold nanoparticle surface so that the overall charge in layer around gold nanoparticles becomes close to neutral. Then the gold nanoparticles tend to agglomerate easily and particle size will be larger. In case that the pH is in a range of 5.9-7.2, when the zeta potential is in a range of -40 to -60 mV, the added ions are not enough to neutralize the overall charge in layer around gold nanoparticles so that the particles will be fairly stable. In case that the pH is above 9.1, when the zeta potential is lower than -60 mV, the reduction reaction does not occur easily because the addition of a base causes the stepwise substitution of Cl^- ions in the inner sphere of coordination of Au^{3+} by the OH^- ions as shown in equation 5.1 (Goia et al., 2006).

$$AuCl_{5-n}(OH)_{n-1}^- + OH^- \leftrightarrow AuCl_{4-n}(OH)_n^- + Cl^- \qquad (5.1)$$

With this reason, the absorbance could be supposed to be very low under alkaline conditions (higher pH). Nevertheless, little amount of gold nanoparticles can be produced. In such condition, hydroxide ions adsorb on a gold surface immediately after gold particles were produced so that the overall charge in layer around gold nanoparticles becomes more negative. This result suggests that a repulsion force between gold particles becomes higher. Therefore, gold particles will be stable for a long time.
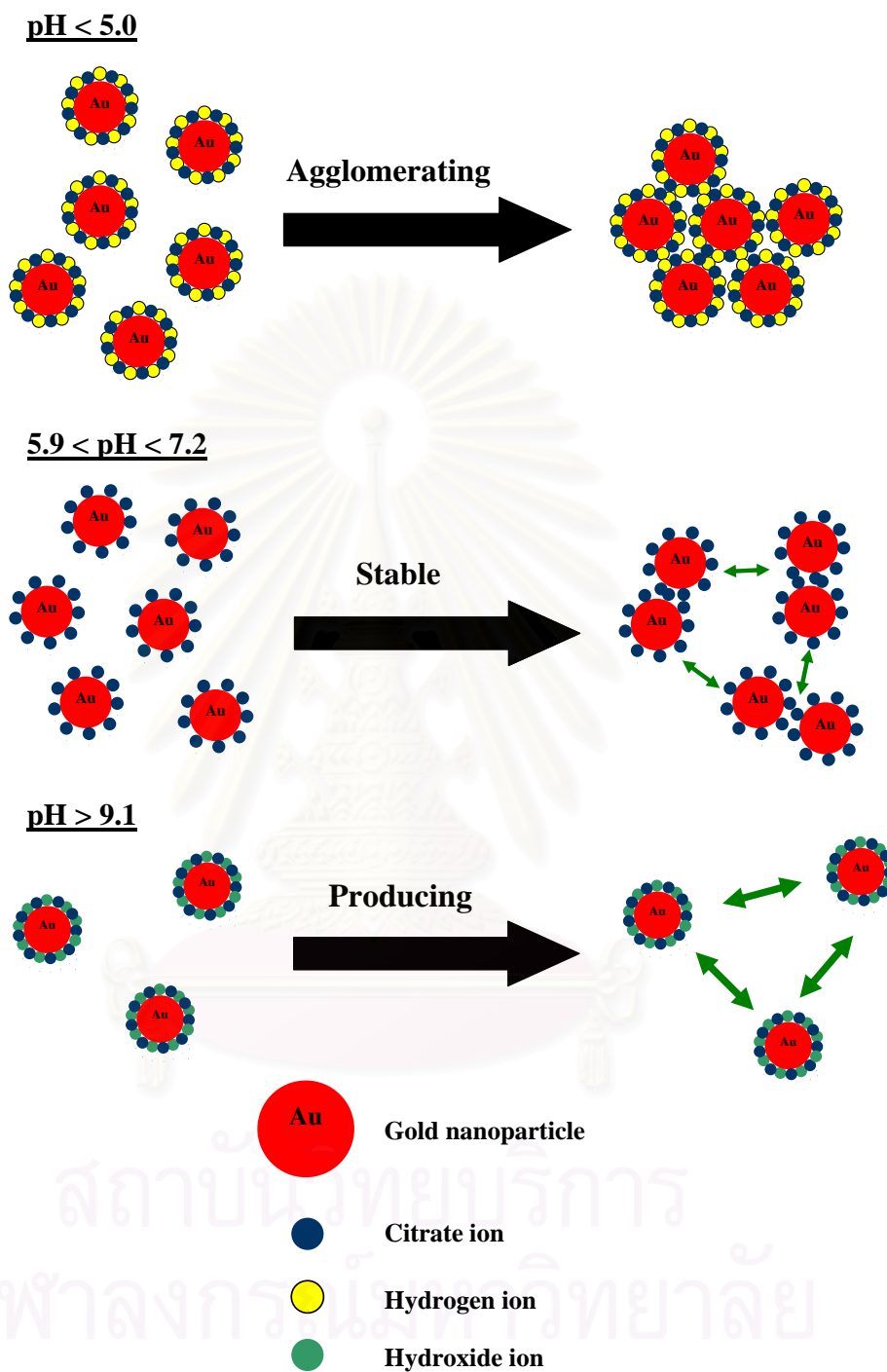
pH < 5.0

Agglomerating

5.9 < pH < 7.2

Stable

pH > 9.1

Producing

Au — Gold nanoparticle

— Citrate ion

— Hydrogen ion

— Hydroxide ion

Figure 5.18 Phenomena of the gold nanoparticle growth under three different conditions

5.6 Comparing sensitivity to ozone gas among CNTs sensor, gold nanoparticles sensor and CNTs-gold nanoparticles sensor

According to good sensing properties and high surface per volume of CNTs and gold nanoparticles, we aimed to look into possibility to combine CNTs and gold nanoparticles for using as ozone sensor using the sensor fabrication method described in previous chapter. Based on our experimental results, a change of resistance of CNTs-gold nanoparticles sensor was shown in Figure 5.19. An electrical resistance of this sensor decreased immediately after supplying ozone to system and increased gradually until the termination of supplying ozone. To analyze this phenomenon, we fabricated CNTs sensor and gold nanoparticles sensor to compare the sensitivity of both sensors. It was found that an electrical resistance of CNTs sensor (Figure 5.20) decreased immediately after supplying ozone gas to a system and became stable after supplying ozone for 120 seconds. After termination of supply ozone gas, a resistance increased gradually due to desorptions of an ozone gas. This phenomenon can be explained by a transfer of charges between CNTs and ozone. The electrical resistance of the CNTs-film decreases with the adsorption of ozone molecules thereon due to electron transfer from the ozone molecules to surface of CNTs (Sano and Ohtsuki, 2007). On the other hand, gold nanoparticles sensor (Figure 5.21) displays contrary phenomenon. Ozone decomposes to oxygen on the gold surface and electrons transfer from gold to the oxygen layer (Pacey et al., 2005), leading to an increase in electrical resistance. Due to contrary phenomena of electron transfer, it is possible to explain a phenomenon in Figure 5.19 that a decrease in an electrical resistance after supplying ozone occurs because of a transfer of electron from ozone molecules to CNTs surface.

It should be noted that a gradual increase in electrical resistance when supplying ozone is caused by a transfer of electron from gold nanoparticles to oxygen layer.
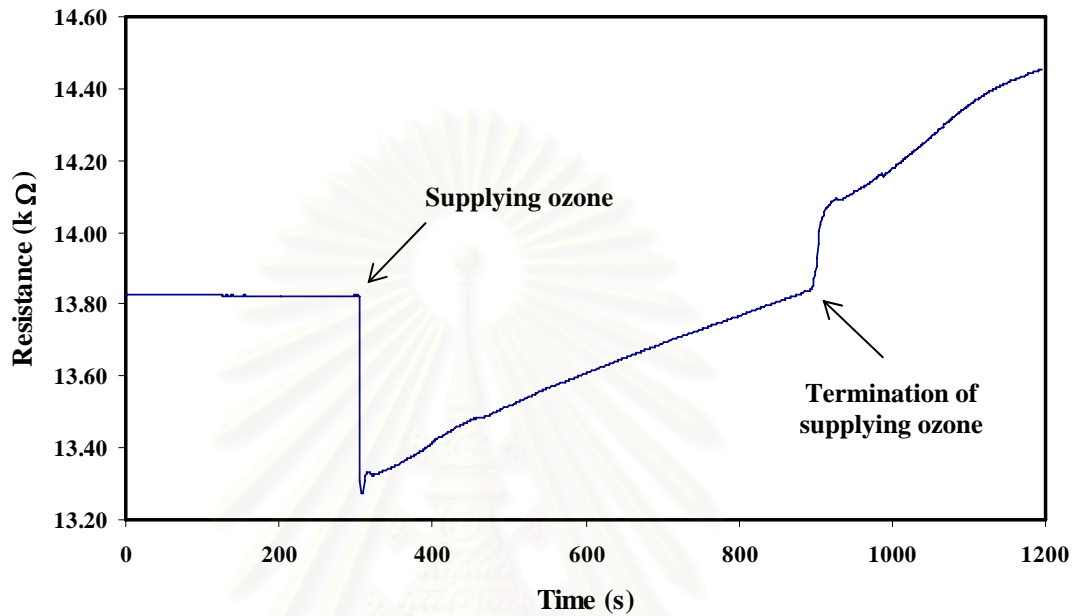

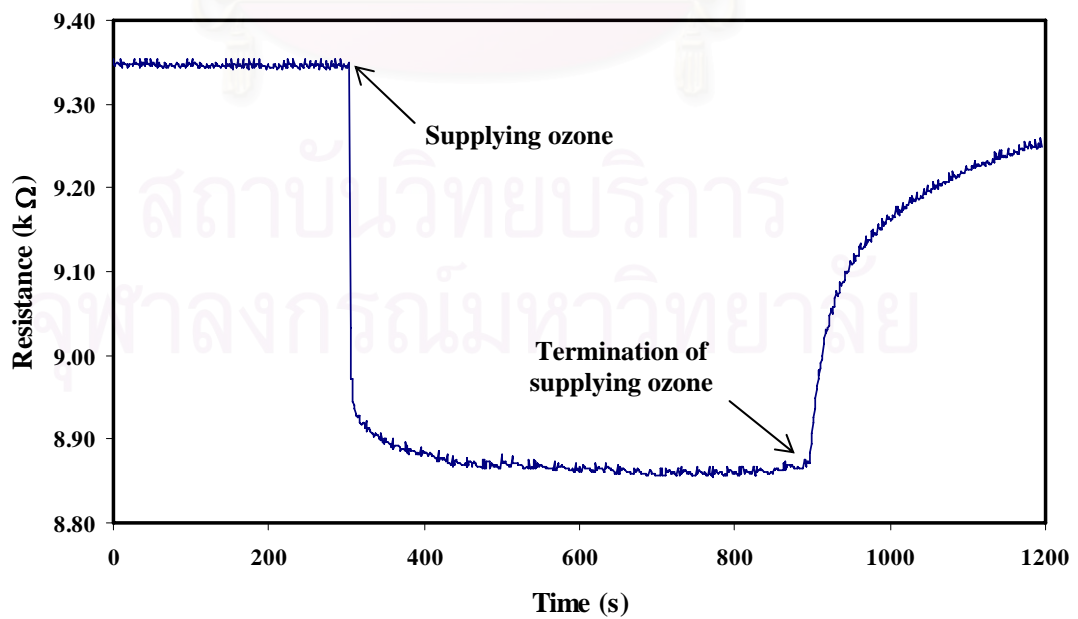**Figure 5.19** Change of electrical resistance of CNTs-gold nanoparticles sensor

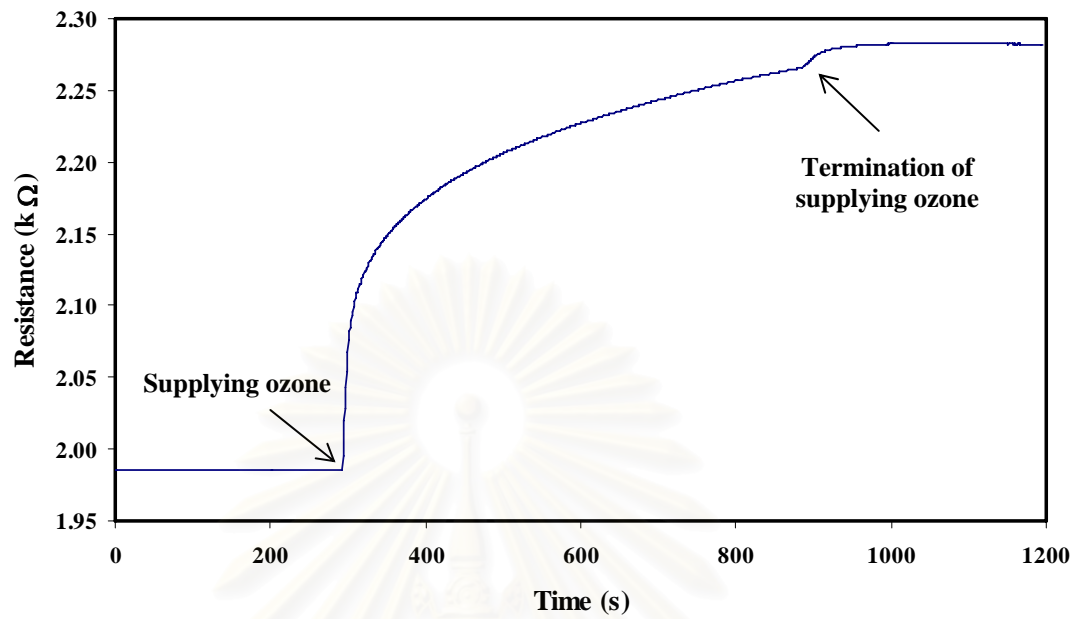**Figure 5.20** Change of electrical resistance of CNTs sensor

Figure 5.21 Change of electrical resistance of gold nanoparticles sensor

CHAPTER VI

CONCLUSIONS AND RECOMMENDATIONS

6.1   Conclusions

6.1.1 Effect of molar ratio of precursor to reducing agent

It was experimentally found that the size of gold nanoparticle was strongly dependent on molar ratio of $HAuCl_4$ to $Na_3C_6H_5O_7$. An amount of sodium citrate played an important role in the formation of gold nanoparticles. We found that the smallest gold nanoparticles (16 nm) were prepared when molar ratio was 1:5. Under conditions of lower molar ratio (1:1 or 1:2), sodium citrate as the electron donor would not be sufficient to react with $HAuCl_4$, resulting in an agglomeration of synthesized gold nanoparticles owing to the van der waal interaction. On the other hand, with the increased molar ratio of sodium citrate the excessive reducing agents would be adsorbed on the surface of synthesized gold nanoparticles, resulting in a decrease in the surface charge of the nanoparticles, which causes the reversible coagulation of the nanoparticles

6.1.2 Effect of total concentration of reactants

An increase in total concentrations of precursors resulted in a red shift of MAW to longer wavelength, referring to the larger gold product. An increase in gold nanoparticles synthesized in the system would be attributed to the increasing rate of collision, leading to the agglomeration of the particles in the system.

6.1.3 Effect of reaction temperature

Two possible explanations were proposed to discuss the effect of reaction temperature on size of synthesized gold nanoparticles. For the first possibility, a decrease in reaction temperature led to larger size of gold nanoparticles because the concentration of a solute in solvent would exceed its equilibrium solubility. The overall energy of the system would be reduced by segregating solute from the solution. The other possibility to explain this phenomenon is the lower density of solvent by increasing temperature. With the larger volume, a number of collisions among particles will decrease, resulting in smaller obtained size of nanoparticles.

6.1.4 Effect of sonication power

Based on our experimental results, an increase in sonication power provided negligible effect on MAW of synthesized products. It would be implied that the ultilization of ultrasonic equipment available in our laboratory would not provide sonication power sufficient to decrease the size of synthesized gold nanoparticles.

6.1.5 Effect of pH

The sizes and stabilities of gold nanoparticles are strongly dependent on the overall charge of interfacial zone at particle surface. The charges of gold nanoparticles could be controlled by adjusting pH of the precursor solution. It is experimentally found that when pH of the solution of $HAuCl_4$ and $Na_3C_6H_5O_7$ is controlled by introducing either NaOH or HCl with different concentration, the zeta potential of suspension of gold nanoparticles changes accordingly. With pH in a range of 5 to 9, the solution zeta potential is in a range of -40 to -60 mV, resulting in a stable

red suspension of gold nanoparticles. Under a condition with pH <5, gold nanoparticles start to agglomerate after being kept quiescently for days due to an adsorption of H^+ on a gold surface, which in turn enhances the attractive van der waals force among particles. Meanwhile, it becomes more difficult to synthesize stable gold nanoparticles with pH >9 because of the stepwise substitution of Cl^- by the OH^- in gold chloride compound. Additionally, the adsorption of OH^- on the surface of synthesized gold nanoparticles leads to better dispersion due to an electrostatic repulsion force, which may inhibit the growth of gold nanoparticles.

6.1.6 Comparing sensitivity to ozone gas among CNTs sensor, gold nanoparticles sensor and CNTs-gold nanoparticles sensor

Three kinds of sensor displayed different sensitivity to ozone gas. For CNTs sensor, the electrical resistance of the CNTs-film decreases with the adsorption of ozone molecules due to electron transfer from the ozone molecules to surface of CNTs. On the other hand, gold nanoparticles sensor, an increase of electrical resistance due to electron transfer from gold to the oxygen layer, which decomposed from ozone. CNTs-gold nanoparticles sensor displayed both attributes of CNTs and gold. However, sensitivity of this sensor became worse comparing with CNTs sensor and gold sensor.

6.2   Recommendations

Due to high surface area of nanoparticles, gold nanoparticles are still of interest for ozone and others sensor applications. Gold nanoparticles sensors made from different size of gold nanoparticles such as 15 nm (from molar ratio = 1:5), 37 nm (from molar ratio =1:2), 45 nm (from molar ratio =1:1) and bulk gold should be further investigated. It is possible that smaller size of gold is more sensitive to ozone because of higher surface area.
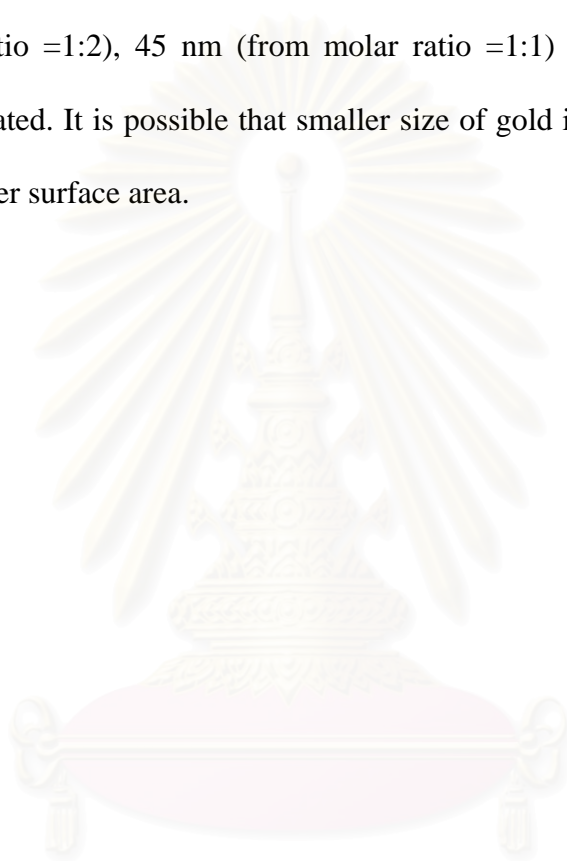
REFERENCES

Atobe, M.; Park, J.E.; and Fuchigami, T. Synthesis of multiple shapes of gold nanoparticles with controlled sizes in aqueous solution using ultrasound. Ultrason. Sonochem. 13 (2006): 237-241

Bhattacharya, S.; and Srivastava, A. Synthesis of gold nanoparticles stabilised by metal-chelator and the controlled formation of close-packed aggregates by them. Proceedings of Indian Acad. Sci. (Chem. Sci.) 115 (October 2003): 613–619

Brust, M.; Walker, M.; Bethell, D.; Schiffrin, D.J.; and Whyman, R. Synthesis of thiol-derivatized gold nanoparticles in a two phase liquid-liquid system. J. Chem. Soc. Chem. Commun. (1994): 801-802.

Cao, G. Nanostructure & Nanomaterials: Synthesis, properties & Applications. Imperial College Press (2004)

Chow, M.K; Zukoski, C.F.; Grieser, F. The Role of Colloidal Stability in the Formation of Gold Sols. J. Colloid Interf. Sci. 160 (1993): 511-513

Corti, C.W.; Holliday, R.J. ; and Thompson D.T., The unique properties of gold for nanoscale technologies and fabrication, presented at the 1st Nanofabrication Symposium, 10-12 March, 2004, Dundalk, Ireland

Dai, S.; Zhu, H.; Pan, Z.; Hagaman, E.W.; Liang, C.; and Overbury, S.H. Facile one-pot synthesis of gold nanoparticles stabilized with bifunctional amino/siloxy ligands. J. Colloid Interface Sci. 287 (2005): 360–365

Dravid, V.P.; Aslam, M.; Fu, L.; Su, M.; and Vijayamohanan, K.; Novel one-step synthesis of amine-stabilized aqueous colloidal gold nanoparticles. J. Mater. Chem. 4 (2004): 1795–1797

Dutta, J.; and Sugunan, A. Novel synthesis of gold nanoparticles in aqueous media. Proceedings of MRS, fall 2005 conference. Boston

Dutta, J.; Sugunan, A.; Thanachayanont, C.; and Hilborn, J.G.; Heavy-metal ion sensors using chitosan-capped gold nanoparticles. STAM 6 (2005): 335–340

Everett, D.H. Basic Principles of Colloid Science. Royal Society of Chemistry (1988)

Frens, G. Controlled nucleation for the regulation of the particle size in monodisperse gold suspensions. Nature Phys. Sci. 241 (1973): 20-22

Goia, D.V.; Andreescu, D.; and Sau, T.K. Stabilizer-free nanosized gold sols. J. Colloid Interface Sci. 298 (2006): 742-751.

Henglein, A.; and Meisel, D. Radiolytic control of the size of colloidal gold nanoparticles. Langmuir 14 (1998): 7392-7396

Holdich, R.G. Fundamental of Particle Technology. Midland Information Technology and Publishing, ISBN 0-9543881-0-0

Hosokawa, M.; Nogi, K.; Naito, M.; and Yokoyama, T.; Nanoparticle Technology Handbook. Elsevier (2007)

Huang, H.; and Yang, X.; Shape control synthesis of gold nanoparticles stabilized by 3-thiopheneacetic acid. Colloids and Surfaces A: Physicochem. Eng. 255 (2005): 11-17

Hunter, R.J. Introduction to Modern Colloid Science. Oxford University Press (1993)

Khanna, P.K.; Gokhale, R.; Subbarao, V.V.V.S.; Vishwanath, A.K.; Das, B.K.; and Satyanarayana, C.V.V. PVA stabilized gold nanoparticles by use of unexplored albeit conventional reducing agent. Mater. Chem. Phys. 92 (2005): 229–233

Lin, H.M.; Lung, J.K.; Huang, J.C.; Tien, D.C.; Liao, C.Y.; Tseng, K.H.; Tsung, T.T.; Kao, W.S.; Tsai, T.H.; Jwo, C.S.; and Stobinski, L. Preparation of

gold nanoparticles by arc discharge in water. <u>J.Alloys and Comp.</u> 434-435 (2007): 655-658

Luo, Y. One-step preparation of gold nanoparticles with different size distribution. <u>Mater. Lett.</u> 61 (2007): 1039-1041

Mareno-Mañas, M.; Pleixats, R.; and Tristany, M. Gold nanoparticles entrapped in heavily fluorinated compounds. <u>J. Fluorine Chem.</u> 126 (2005) 1435-1438

Okubo, T.; Hu, M.; and Yamaguchi, Y. Self-assembly of water-dispersed gold nanoparticles stabilized by a thiolated glycol derivative. <u>J. Nanopart. Res.</u> 7 (2005): 187-193

Pacey, G.E.; Puckett, S.D.; Heuser, J.A.; Keith, J.D.; Spendel, W.U. Interaction of ozone with gold nanoparticles. <u>Talanta</u> 66 (2005): 1242-1246

Pal, T.; Pal, A.; and Esumi, K. Preparation of nanosized gold particles in a biopolymer using UV photoactivation. <u>J. Colloid Interface Sci.</u> 288 (2005): 396–401

Pal, T.; Pal, A.; Jana, N.R.; Wang, Z.L. and Sau, T.K. Size controlled synthesis of gold nanoparticles using photochemically prepared seed particles. <u>J. Nanopart. Res.</u> 3 (2001): 257–261

Pal, T.; Pal, A.; Kundu, S.; Panigrahi, S.; Praharaj, S.; Basu, S.; and Ghosh, S.K. Anisotropic growth of gold clusters to gold nanocubes under UV irradiation. Nanotechnology 18 (2007): 075712 (7pp)

Sano, N.; Ohtsuki, F. Carbon nanohorn sensor to detect ozone in water. J. Electrostat. 65 (2007): 263–268

Sastry, M.; Mandal, S.; Selvakannan, P.R.; Phadtare, S.; and Pasricha, R. Synthesis of a stable gold hydrosol by the reduction of chloroaurate ions by the amino acid, aspartic acid. Proceedings of Indian Acad. Sci. (Chem. Sci.) 114 (October 2002): 513–520

Scaffardi, L.B.; Pellegri, N.; de Sanctis, O.; and Tocho, J.O. Sizing gold nanoparticles by optical extinction spectroscopy. Nanotechnology 16 (2005): 158–163

Song, J.H.; Kim, Y.J.; and Kim, J.S. Synthesis of gold nanoparticles using N, N-dimethylacetoacetamide: Size and shape control by the reaction temperature. Curr. App. Phys. 6 (2006): 216–218

Toshima, N.; Shiraishi, Y.; and Arakawa, D. pH-dependent color change of colloidal dispersions of gold nanoclusters: Effect of stabilizer. Eur. Phys. J. E 8 (2002): 377–383

Turkevitch, J.; Stevenson, P.C.; and Hillier, J.; Nucleation and growth process in the synthesis of colloidal gold. Discuss. Faraday Soc. 11 (1951): 55-75

Yonezawa, T.; and Kunitake, T. Practical preparation of anionic mercapto ligand-stabilized gold nanoparticles and their immobilization, Colloids Surf. A: Physicochem. Eng. Asp. 149 (1999): 193-199.

Wang, L.; Jiang, G.; Chen, T.; Yu, H.; and Chen, C. Preparation of gold nanoparticles in the presence of poly (benzyl ether) alcohol dendrons. Mater. Chem. Phys. 98 (2006) 76-82

APPENDIX A

CVD method and Calibration graph for sonication power

APPENDIX A1

Synthesis of CNTs on silicon wafer by CVD method

Experimental apparatus for synthesis of CNTs on silicon wafer is shown in Figure A1. The condition to synthesize CNTs is shown below:

Step 1: H_2: 25 mL/min

Reaction temperature: 400 ^{O}C

Reaction time: 30 minutes

Step 2: C_2H_4 : 30 mL/min

H_2: 15 mL/min

Reaction temperature: 850 ^{O}C

Reaction time: 10 minutes

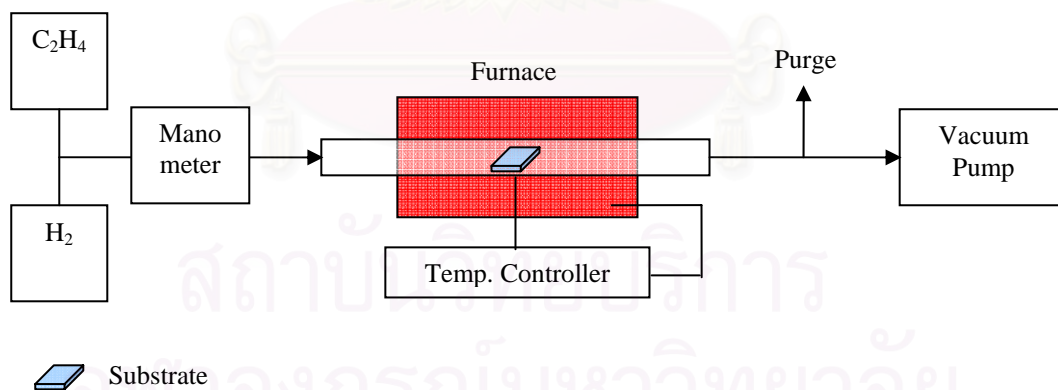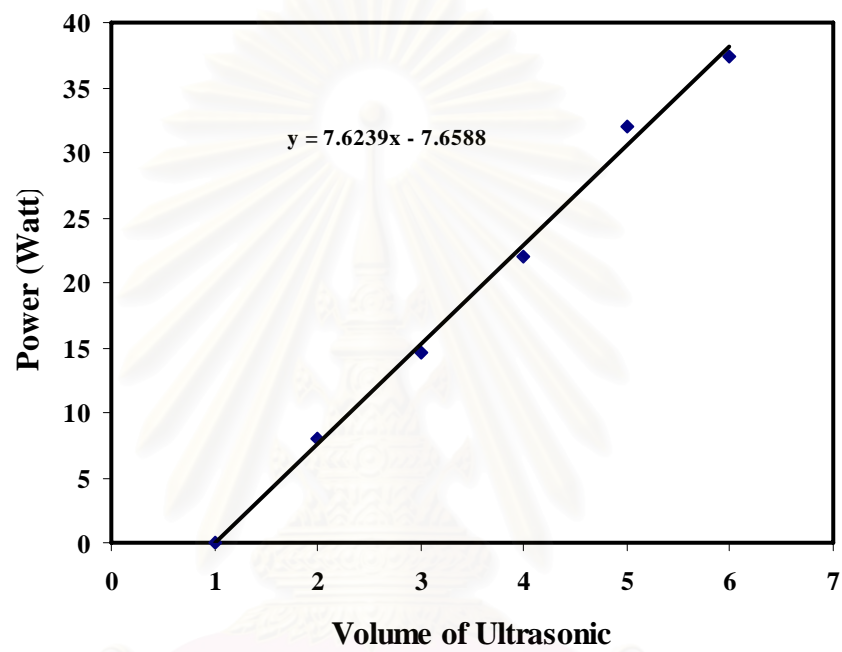**Figure A1** Experimental apparatus to synthesize CNTs on silicon wafer

APPENDIX A2

Calibration graph for ultrasonic homogenizer

$y = 7.6239x - 7.6588$

Level	Power (W)
1	0.0
2	7.6
3	15.2
4	22.8
5	30.5
6	38.1

Figure A2 Calibration curve of Ultrasonic Homogenizer
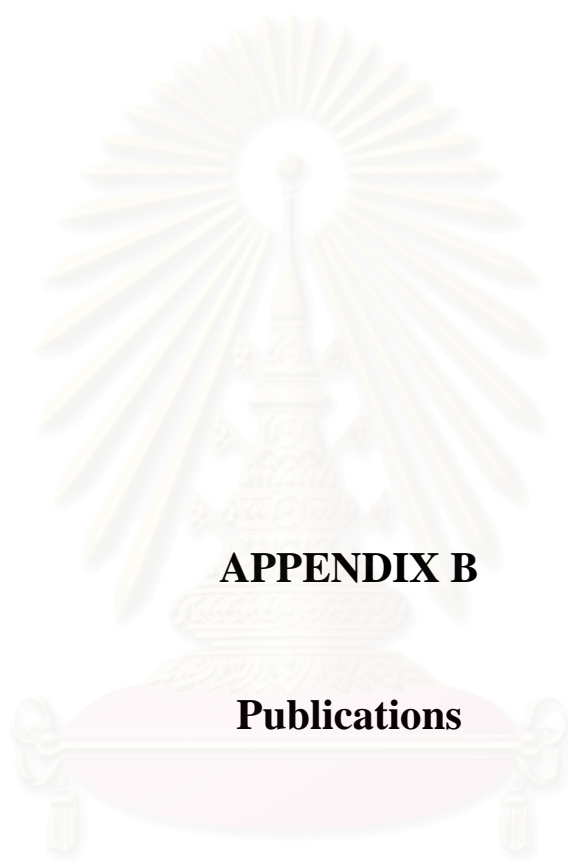
APPENDIX B

Publications

PUBLICATIONS

International Proceedings

1. **T. Muangnapoh,** N. Viriya-empikul, T. Charinpanitkul, and N. Sano, "Effect of pH on stability of gold nanoparticles synthesized by aqueous reaction" *Proceedings of Regional Symposium on Chemical Engineering (RSCE 2007),* December 4-5, 2007, Yogyakarta, Indonesia.

2. T. Charinpanitkul, **T. Muangnapoh,** N. Viriya-empikul, and N. Sano, "Stability control of gold nanoparticles synthesized by wet chemistry," *Proceedings of the 5th Eco-Energy and Materials Science and Engineering Symposium (5th EMSES),* November 21 - 24, 2007, Pattaya, Thailand.

Domestic Proceedings

1. **T. Muangnapoh,** N. Viriya-empikul, T. Charinpanitkul, and N. Sano, "Size-controllable synthesis of gold nanoparticles by wet chemistry" *Proceedings of Thailand Research Fund-Master Research Grants Congress II*, April 4-6, 2008, Pattaya, Thailand.

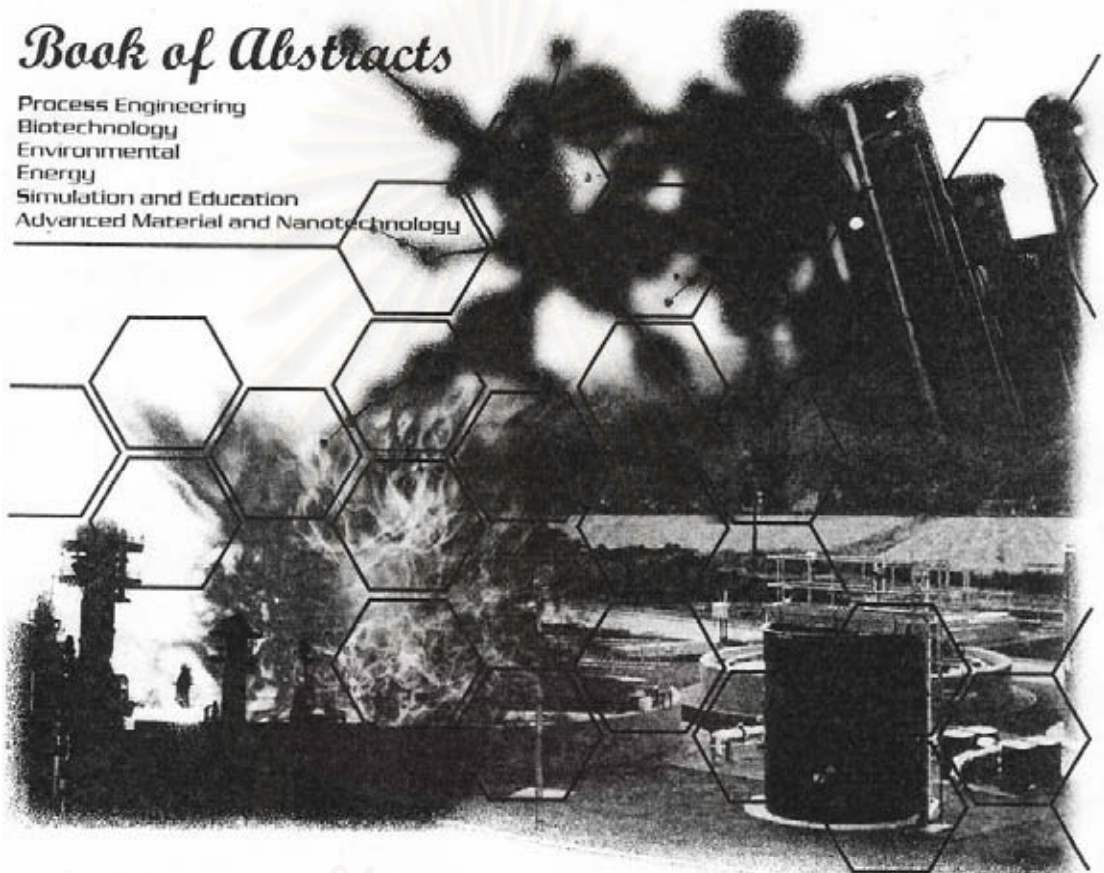December 4 - 5, 2007
Melia Purosani Hotel
Yogyakarta - Indonesia

RSCE

Regional Symposium on Chemical Engineering

Book of Abstracts

Process Engineering
Biotechnology
Environmental
Energy
Simulation and Education
Advanced Material and Nanotechnology

Organized by
Gadjah Mada University Chemical Engineering Dept.

Sponsored by

KMI
Kaltim Methanol Industri

Chevron

PERTAMINA
Always There

Effect of pH on stability of gold nanoparticles synthesized by aqueous reaction

T. Muangnapoh[a,*], N. Viriya-empikul[a], T. Charinpanitkul[a] and N. Sano[b]

[a] Center of Excellence in Particle Technology, Faculty of Engineering, Chulalongkorn University, Thailand
[b] Department of Mechanical and System Engineering, Faculty of Engineering, University of Hyogo, Japan

ABSTRACT

The sizes and stabilities of gold nanoparticles are strongly dependent on the overall charge of interfacial zone at particle surface. The charges of gold nanoparticles are controlled by adjusting pH of the precursor solution. It is experimentally found that when pH of the solution of $HAuCl_4$ and $Na_3C_6H_5O_7$ is controlled by introducing either NaOH or HCl with different concentration, the zeta potential of suspension of gold nanoparticles changes accordingly. With pH in a range of 5 to 9, the solution zeta potential is in a range of -40 to -60 mV, resulting in a stable red suspension of gold nanoparticles. Under a condition with pH <5, gold nanoparticles start to agglomerate after being kept quiescently for a day due to an adsorption of H^+ on a gold surface, which in turn enhances the attractive van der waals force among particles. Meanwhile, it becomes more difficult to synthesize stable gold nanoparticles with pH >9 because of the stepwise substitution of Cl^- by the OH^- in gold chloride compound. Additionally, the adsorption of OH^- on the surface of synthesized gold nanoparticles leads to better dispersion due to an electrostatic repulsion force, which may inhibit the growth of gold nanoparticles.

Keywords: gold nanoparticle, pH, stability, zeta potential

* e-mail : t_muangnapoh@hotmail.com

1. Introduction

Nowadays, metal nanoparticles have become of interest because their extraordinary physical and chemical properties are different from that of bulk. One of the most interesting substances is gold. In its bulk form, gold is the most stable metal substances which is inert, soft, yellow metal, having a face centered cubic structure with a melting point of 1068 $^{\circ}$C [1]. At the nanoscale, gold nanoparticles show different color appearance and provide many potential applications in electronics, catalysis and biomedical fields.

There are many ways to synthesize gold nanoparticles such as thermal decomposition [2], sol-gel [3], photolysis [4] and radiolysis [5]. Nevertheless, these methods require sophisticated apparatus.

However, there are two well-known methods that employ less energy and simple apparatus. The First one is Turkevitch method. It is a conventional technique for synthesis of aqueous gold nanoparticles by the reduction reaction of Auric chloride with trisodium citrate which was proposed by Turkevitch [6] in 1951. With this method, the citrate salt acts as the reducing agent to reduce Au^{3+} to Au^{0} and then it also acts as the stabilizing agent by forming a layer of citrate ions over gold nanoparticles surface, inducing enough electrostatic repulsion between individual particles to keep them well dispersed in the medium. For this method, reducing agents play an important role as a reducer and an electrostatic stabilizer at the same time. A particle size obtained is about 20 nm. This method gives uniform and fairly spherical nanoparticles. The second one is Brust-Schiffrin method. This method was discovered by Brust and Schifrinn [7] in 1994. They produced gold nanoparticles in organic liquids that are normally not miscible with water (two-phase synthesis) with thiols as a stabilizer. Nanoparticles show that they have diameters in range of 1-3 nm and a maximum particle size distribution at 2.0-2.5 nm. However, nanoparticles prepared by this method cannot be used in wide applications due to existence of functionalized thiols on gold surface.

After that, there are many reports that investigated in this field. Many reducing agents were investigated such as sodium borohydride [7], ascorbic acid [8], aspartic acid [9], and so forth.

To the best of our knowledge, many researchers have studied only on the formulation of gold nanoparticles but the stability of gold nanoparticles solution has not been thoroughly investigated. In such situation, this research will investigate the stability of gold nanoparticles colloid with measuring zeta potential and absorption spectrum of colloid. The benefit of this research is to improve a stability of gold colloid because an aggregation of gold nanoparticles will not occur if there is an optimal condition is prepared to add a suitable amount of ions around particles.

2. Experimental

2.1 Materials

Gold (III) chloride trihydrate ($HAuCl_4.3H_2O$), tri-sodium citrate, 2-hydrate ($Na_3C_6H_5O_7.2H_2O$), hydrochloric acid (HCl) and sodium hydroxide (NaOH) were purchased from Sigma-Aldrich and Kishida. All reagents were prepared according to procedures below.

2.2 Preparation of gold nanoparticles solution

1 ml of 2.03×10^{-2} mol dm^{-3} aqueous solution of $HAuCl_4$ and 1 ml of 10.16×10^{-2} mol dm^{-3} aqueous solution of sodium citrate were used for every condition. For condition (1), neither NaOH nor HCl was added. In an attempt to vary the pH of gold nanoparticles solution (pH= 3.1-10.1), 1 ml each of (2) 5×10^{-3}, (3) 1.0×10^{-2}, (4) 1.5×10^{-2}, (5) 2.0×10^{-2}, (6) 2.5×10^{-2} mol dm^{-3} of NaOH and (7) 2.5×10^{-3}, (8) 1.0×10^{-2}, (9) 2.0×10^{-2}, (10) 3.0×10^{-2}, (11) 4.0×10^{-2} mol dm^{-3} of HCl were required. All conditions were diluted into 10 ml and reacted at a boiling temperature for 10 minutes.

2.3 Characterization of gold nanoparticles solution

Ultraviolet and visible (UV-Vis) spectra were obtained at room temperature using a UV-visible spectrophotometer (Shimadzu UV-1600PC). The zeta potential of the gold nanoparticles was measured using a dynamic light scattering analyzer (Zetasizer 3000 HS_A, Malvern). Before measurements, sediment is separated by a centrifuge for 30 minutes.

3. Results and discussions

The pH of the gold nanoparticle solution was adjusted by varying hydrochloric acid (HCl) or sodium hydroxide solution (NaOH). The pH and absorption spectra of each gold nanoparticle solution are shown in Table1. In Fig.1 showing the relationship between pH and zeta potential, the zeta potentials directly vary to pH of solution. This phenomenon is attributable to the adsorption of the OH^- and H^+ ions on the surface of gold nanoparticles and then the particle surface charge density is changed.

Table1. pH of prepared solution and a photo absorbance characteristic of the products

Condition No.	pH	Maximum absorption wavelength (nm)
1	6.2 ± 0.04	518.5
2	6.8 ± 0.1	518.5
3	7.2 ± 0.1	534
4	9.1 ± 0.5	-
5	9.8 ± 0.3	-
6	10.1 ± 0.1	-
7	5.9 ± 0.1	519.5

8	5.0 ± 0.1	527.0
9	3.9 ± 0.1	540.0
10	3.4 ± 0.1	564
11	3.1 ± 0.1	-

As seen in Figs.2-4, there are 3 types of results. In the first one, when pH is below 5.0, the stability of solution becomes the worse. Particles tend to agglomerate faster than the condition no.1, non-treated solution. In the second one, when pH is in a range of 5.9-7.2, the stability looks very high. For such situations, the absorbance is constant for a long time. In the last one, when pH is above 9.1, the reaction occurs slowly. Their absorbance increases by every week.

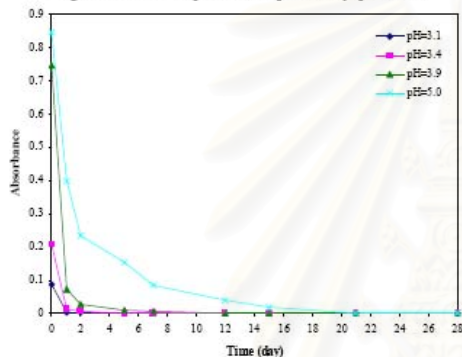Fig.1 a relationship between pH and ξ -potential

Fig.2 Change of absorbencies in the condition when pH is below 5.0
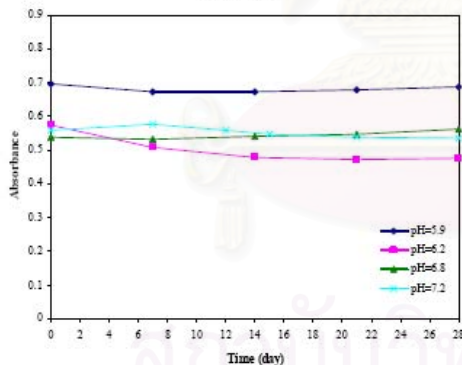

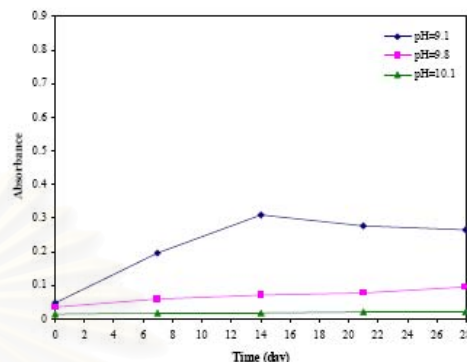Fig.3 Change of absorbencies in the condition when pH is in a range of 5.9-7.2

Fig.4 Change of absorbencies from in the condition when pH is above 9.1

Form these results, we can conclude that the rate of agglomeration will be faster if the pH is lower. This phenomenon can be explained in Fig.5. For the case when pH is below 5.0 with the zeta potential higher than -40 mV, a lot of added hydrogen ions in the solution adsorb on a gold surface so that the overall charge in layer around gold nanoparticles becomes close to neutral. Then the gold nanoparticles tend to agglomerate easily and particle size will be larger. In case that the pH is in a range of 5.9-7.2, when the zeta potential is in a range of -40 to -60 mV, the added ions are not enough to neutralize the overall charge in layer around gold nanoparticles so that the particles will be fairly stable. In case that the pH is above 9.1, when the zeta potential is lower than -60 mV, the reduction reaction does not occur easily because the addition of a base causes the stepwise substitution of Cl$^-$ ions in the inner sphere of coordination of Au^{3+} by the OH$^-$ ions [8]. For this reason, the absorbance will be very low at a high pH condition. Nevertheless, little amount of gold nanoparticles can be produced. In such condition, hydroxide ions adsorb on a gold surface immediately after gold particles were produced so that the overall charge in layer around gold nanoparticles becomes more negative. It means that a repulsion force between gold particles becomes higher. So, gold particles will be smaller and stable for a long time.

Conclusion

The overall charges around gold nanoparticles play an important role in their stability. In this research, we adjust the charge accumulated on gold particle surface by varying pH. As a result, there are three kinds of possible phenomena taking place while gold nanoparticles are formed. An agglomeration of primary particles will occur in a condition that the zeta potential is close to 0 mV. While the stable gold nanoparticles can be synthesized in a suitable condition, when the zeta

potential is in a range of -40 to -60 mV. For the zeta potential lower than -60 mV, gold nanoaparticles are produced slowly with a long growth time and then stabilized immediately after their formation.
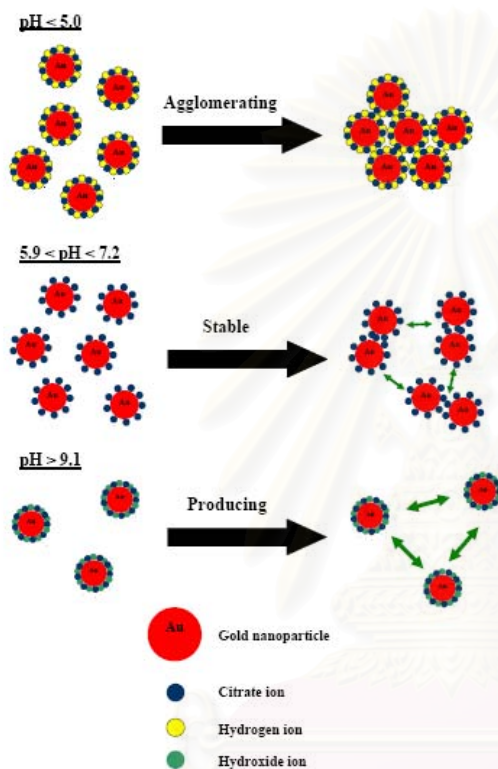
pH < 5.0

5.9 < pH < 7.2

pH > 9.1

Au — Gold nanoparticle

● — Citrate ion

○ — Hydrogen ion

● — Hydroxide ion

Fig.5 Phenomena of the gold nanoparticle growth under three different conditions

References

[1] C.W. Corti, R.J. Holliday and D.T. Thompson, The unique properties of gold for nanoscale technologies and fabrication, presented at the 1st Nanofabrication Symposium, 10-12 March, 2004, Dundalk, Ireland

[2] D. Wostek-Wojciechowska, J. K. Jeszka, C. Amiens, B. Chaudret, P.Lecante, The solid-state synthesis of metal nanoparticles from organnometallic precursors, Journal of Colloid and Interface Science, 287 (2005), page 107-113

[3] M. Epifani, C. Giannini, L. Tapfer, L. Vasanelli, Sol-Gel Synthesis and Characterization of Ag and Au Nanoparticles in SiO_2, TiO_2 and ZrO_2 Thin Films, J. Am. Ceram. Soc., 83(2000), page 2385-2393

[4] A.Pal, K. Esumi, T. Pal, Preparation of nanosized gold particles in a biopolymer using UV photoactivation, Journal of Colloid and Interface Science 288 (2005) 396–401

[5] M.C. Daniel, D. Astruc, Gold Nanoparticles: Assembly, Supramolecular Chemistry, Quantum-Size-Related Properties, and Applications toward Biology, Catalysis, and Nanotechnology, Chem. Rev. 2004, 104, 293-346

[6] J. Turkevitch, P.C. Stevenson, J. Hillier, Nucleation and Growth Process in the Synthesis of Colloidal Gold. Discuss. Faraday Soc. 1951, 11, page 55-75

[7] M. Brust, M. Walker, D. Bethell, D. J.Schiffrin, R. J. Whyman, Synthesis of Thiol-Derivatized Gold Nanoparticles in a Two phase Liquid-Liquid System. J. Chem. Soc., Chem. Commun. 1994, page 801-802.

[8] D. Andreescu, T. K. Sau, D. V. Goia, Stabilizer-free nanosized gold sols, Journal of Colloid and Interface Science 298 (2006),page 742-751.

[9] S. Mandal, P.R. Selvakannan, S. Phadtare, R. Pasricha, M. Sastry, Synthesis of a stable gold hydrosol by the reduction of chloroaurate ions by the amino acid, aspartic acid, Proc. Indian Acad. Sci. (Chem. Sci.), Vol. 114, No.5, October 2002, page 513–520

Stability control of gold nanoparticles synthesized by wet chemistry

T. Charinpanitkul[1], T. Muangnapoh[1], N. Viriya-empikul[1], and N. Sano[2]

[1]Center of Excellence in Particle Technology, Faculty of Engineering, Chulalongkorn University, Thailand
[2]Department of Mechanical and System Engineering, Faculty of Engineering, University of Hyogo, Japan

Abstract: Synthesis of gold nanoparticles using wet chemistry method has been investigated experimentally. It is found that particle stability and sizes are strongly dependent on the overall charge accumulated on the particle surface. In order to avoid particle agglomeration, electrostatic charges of gold nanoparticles are controlled by adjusting pH of the precursor solution of $HAuCl_4$. Either NaOH or HCl with different concentration are added to control pH of the solution of $HAuCl_4$ and $Na_3C_6H_5O_7$, resulting in significant changes of the zeta potential of gold nanoparticles suspensions. With pH in a range of 5 to 9, the solution zeta potential is in a range of -40 to -60 mV, leading to a stable red suspension of gold nanoparticles. On the other hand, under a condition with pH <5, gold nanoparticles start to agglomeration of gold nanoparticles becomes more enhanced. It is attributed to an adsorption of H^+ on the gold nanoparticle surface, which in turn enhances the attractive van der waals force among particles. Meanwhile, in a system using HCl, the synthesized gold nanoparticles become less stable with pH >9 because of the stepwise substitution of Cl^- by OH^-. However, a further increase in OH^- adsorption on the surface of synthesized gold nanoparticles leads to better dispersion due to an electrostatic repulsion force, which inhibit the agglomeration of gold nanoparticles.

Keywords: gold nanoparticle, pH, stability, zeta potential

Size-controllable synthesis of gold nanoparticles by wet chemistry

Tanyakorn Muangnapoh[1], N. Viriya-empikul[1], Tawatchai Charinpanitkul[1] and Noriaki Sano[2]

[1] Center of Excellence in Particle Technology, Faculty of Engineering, Chulalongkorn University
[2] Department of Mechanical and System Engineering, Faculty of Engineering, University of Hyogo

Introduction and Objective

It has been known that gold is precious metal with very high stability. In nanoscale, gold nanoparticle could exhibit distinctive properties, which are different from its bulk. Optical is the most interesting properties because it is strongly dependence on size of gold nanoparticles which could be controlled by many parameters [1]. Hence this research sets its aim at investigating the dependence of gold nanoparticle size on the molar ratio of precursor and reducing agent.

Methods

Gold (III) chloride trihydrate ($HAuCl_4.3H_2O$) and tri-sodium citrate, 2-hydrate ($Na_3C_6H_5O_7.2H_2O$) are used as reagents. Sodium citrate could provide function as a reducing agent and stabilizing agent simultaneously [2]. The synthesized colloidal solution is analyzed by transmission electron microscopy (TEM) (JIM2010, JEOL), UV-visible spectrophotometry (UV-1600PC, Shimadzu) and dynamic light scattering (Zetasizer 3000 HS_A, Malvern).

Results

UV-vis spectrophotometric analyses are shown in Fig 1. It is found that each product showed different Maximum Absorption Wavelength (MAW), which is related to different particle size [3-4]. With the molar ratio of 1:5 ($HAuCl_4$ to $Na_3C_6H_5O_7$), the lowest MAW (518.5 nm) was obtained, suggesting that the smallest gold nanoparticles could be synthesized.
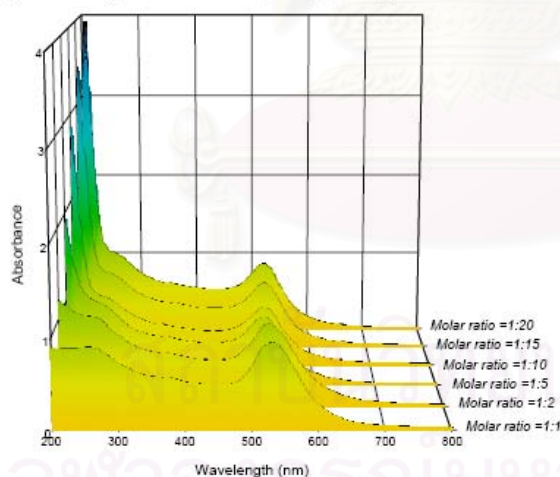

Fig.1 UV-vis spectra of gold nanoparticles synthesized in various molar ratios

Analytical results based on DLS analyses reveal that size of gold nanoparticles synthesized in this work is in a range of 16-45 nm. Such DLS result is in good agreement with the MAW values showing that the smallest particles could be prepared under the condition of 1:5 molar ratio of $HAuCl_4$ to $Na_3C_6H_5O_7$.

Conclusion

It was experimentally found that the size of gold nanoparticle was strongly dependent on molar ratio of $HAuCl_4$ to $Na_3C_6H_5O_7$. Control of certain amount of sodium citrate could result in the formation of gold nanoparticles with desirable size.

Keywords: gold nanoparticle, size, molar ratio, reaction temperature

Selected References:
[1] M.C. Daniel, D. Astruc, Chem. Rev. 2004; 104: 293-346
[2] J. Turkevitch, P.C. Stevenson, J. Hillier, Discuss. Faraday Soc. 1951; 11: 55-75
[3] G. Frens, Nature: Phys. Sci. 1973; 241, 20-22
[4] M.K. Chow, C.F. Zukoski, F. Grieser, J. Colloid Interf. Sci.1993; 160(2), 511-513

VITA

Mr. Tanyakorn Muangnapoh, the first son of Dr. Tirachoon and Dr. Chirakarn Muangnapoh, was born on July 20, 1983 in Toulouse, France. He studied in primary and secondary educations at Chulalongkorn University Demonstration School. In 2005, he received the Bachelor Degree of Engineering (Chemical Engineering) from Chulalongkorn University. After that, he gained admission to Graduate School of Chulalongkorn University and he graduated in 2008 with the thesis entitled "Synthesis of gold nanoparticles using pH control and ultrasonication".